Journal of Visualized Experiments

Magnetic Resonance Imaging of Multiple Sclerosis at 7.0 Tesla

--Manuscript Draft--

Article Type:	Methods Article - JoVE Produced Video
Manuscript Number:	JoVE62142R1
Full Title:	Magnetic Resonance Imaging of Multiple Sclerosis at 7.0 Tesla
Corresponding Author:	Sonia Waiczies Max Delbrück Centre for Molecular Medicine in the Helmholtz Association Berlin, Please select GERMANY
Corresponding Author's Institution:	Max Delbrück Centre for Molecular Medicine in the Helmholtz Association
Corresponding Author E-Mail:	sonia.waiczies@mdc-berlin.de
Order of Authors:	Sonia Waiczies
	Antje Els
	Joseph Kuchling
	Karin Markenroth Bloch
	Anna Pankowska
	Helmar Waiczies
	Carl Herrmann
	Claudia Chien
	Carsten Finke
	Friedemann Paul
	Thoralf Niendorf
Additional Information:	
Question	**Response**
Please specify the section of the submitted manuscript.	Medicine
Please indicate whether this article will be Standard Access or Open Access.	Standard Access (US$2,400)
Please indicate the **city, state/province, and country** where this article will be **filmed**. Please do not use abbreviations.	Berlin, Germany
Please confirm that you have read and agree to the terms and conditions of the author license agreement that applies below:	I agree to the Author License Agreement
Please provide any comments to the journal here.	

TITLE:

Magnetic Resonance Imaging of Multiple Sclerosis at 7.0 Tesla

AUTHORS AND AFFILIATIONS:

Sonia Waiczies[1§], Antje Els[1§], Joseph Kuchling[2,3,4§], Karin Markenroth Bloch[5], Anna Pankowska[6,7], Helmar Waiczies[8], Carl Herrmann[1], Claudia Chien[2,3], Carsten Finke[4,9], Friedemann Paul[2,3,4], Thoralf Niendorf[1,2,8]

[1] Berlin Ultrahigh Field Facility (B.U.F.F.), Max Delbrück Center for Molecular Medicine in the Helmholtz Association

[2] Experimental and Clinical Research Center, Max Delbrueck Center for Molecular Medicine and Charité – Universitätsmedizin Berlin, corporate member of Freie Universität Berlin, Humboldt-Universität zu Berlin, and Berlin Institute of Health, Berlin, Germany

[3] NeuroCure Clinical Research Center, Charité – Universitätsmedizin Berlin, corporate member of Freie Universität Berlin, Humboldt-Universität zu Berlin, and Berlin Institute of Health, Berlin, Germany

[4] Department of Neurology, Charité – Universitätsmedizin Berlin, corporate member of Freie Universität Berlin, Humboldt-Universität zu Berlin, and Berlin Institute of Health, Berlin, Germany

[5] The Swedish National 7T Facility, Lund University Bioimaging Center, Lund University, Lund, Sweden

[6] Department of Radiography, Medical University of Lublin, Lublin, Poland

[7] ECOTECH-COMPLEX, Maria Curie-Skłodowska University, 20-612 Lublin, Poland.

[8] MRI.TOOLS GmbH, Berlin, Germany

[9] Berlin School of Mind and Brain, Humboldt-Universität zu Berlin, Berlin, Germany

[§] Equally contributing

Corresponding Author:

Prof. Dr. Thoralf Niendorf

thoralf.niendorf@mdc-berlin.de

Sonia Waiczies[1§]

sonia.waiczies@mdc-berlin.de

Antje Els[1§]

antje.els@mdc-berlin.de

Joseph Kuchling[2,3,4§]

joseph.kuchling@charite.de

Karin Markenroth Bloch[5]

karin.markenroth_bloch@med.lu.se

Anna Pankowska[6,7]

zubianna@gmail.com

Helmar Waiczies[8]

helmar@waiczies.de

Carl Herrmann[1]
carl.herrmann@mdc-berlin.de

Claudia Chien[2,3]
claudia.chien@charite.de

Carsten Finke[4,9]
carsten.finke@charite.de

Friedemann Paul[2,3,4]
friedemann.paul@charite.de

Thoralf Niendorf[1,2,8]
thoralf.niendorf@mdc-berlin.de

Summary

Here, we present a protocol to acquire magnetic resonance (MR) images of multiple sclerosis (MS) patient brains at 7.0 Tesla. The protocol includes preparation of the setup including the radio-frequency coils, standardized interview procedures with MS patients, subject positioning in the MR scanner and MR data acquisition.

Abstract

The overall goal of this article is to demonstrate a state-of-the-art ultrahigh field (UHF) magnetic resonance (MR) protocol of the brain at 7.0 Tesla in multiple sclerosis (MS) patients. MS is a chronic inflammatory, demyelinating, neurodegenerative disease that is characterized by white and gray matter lesions. Detection of spatially and temporally disseminated T_2-hyperintense lesions by the use of MRI at 1.5 T and 3 T represents a crucial diagnostic tool in clinical practice to establish accurate diagnosis of MS based on the current version of the 2017 McDonald criteria. However, the differentiation of MS lesions from brain white matter lesions of other origins can sometimes be challenging due to their resembling morphology at lower magnetic field strengths (typically $\leq$3 T). Ultrahigh field MR (UHF-MR) benefits from increased signal-to-noise ratio and enhanced spatial resolution, both key to superior imaging for more accurate and definitive diagnoses of subtle lesions. Hence, MRI at 7.0 T has shown encouraging results to overcome the challenges of MS differential diagnosis by providing MS-specific neuroimaging markers (e.g., central vein sign, hypointense rim structures and differentiation of MS grey matter lesions). These markers and others can be identified by other MR contrasts other than T_1 and T_2 (T_2*, phase, diffusion) and substantially improve the differentiation of MS lesions from those occurring in other neuroinflammatory conditions such as neuromyelitis optica and Susac syndrome. In this article, we describe our current technical approach to study cerebral white and grey matter lesions in MS patients at 7.0 T using different MR acquisition methods. The up-to-date protocol includes the preparation of the MR setup including the radio-frequency coils customized for UHF-MR, standardized screening, safety and interview procedures with MS patients, patient positioning in the MR scanner and acquisition of dedicated brain scans tailored for examining MS.

Introduction

Multiple sclerosis (MS) is the most common chronic inflammatory and demyelinating disease of the central nervous system (CNS) that causes pronounced neurological disability in younger adults and leads to long term disability[1,2]. The pathological hallmark of MS is the accumulation of demyelinating lesions that occur in the gray and white matter of the brain and also diffuse neurodegeneration in the entire brain, even in normal-appearing white matter (NAWM)[3,4]. MS pathology suggests that inflammation drives tissue injury at all stages of the disease, even during the progressive stages of disease[5]. The first clinical manifestations of MS are commonly accompanied by reversible episodes of neurological deficits and referred to as a clinically isolated syndrome (CIS), when only suggestive of MS[6,7]. In the absence of a clear-cut CIS, caution should be exercised in making an MS diagnosis: the diagnosis should be confirmed by follow-up and initiation of long-term disease-modifying therapies should be postponed, pending additional evidence[8].

Magnetic resonance imaging (MRI) is an indispensable tool in diagnosing MS and monitoring disease progression[9-11]. MRI at magnetic field strengths of 1.5 T and 3 T currently represents a crucial diagnostic tool in clinical practice to detect spin-spin relaxation time weighted (T_2) hyperintense lesions and establish accurate diagnosis of MS based on the current version of the 2017 McDonald criteria[8]. Diagnostic criteria for MS emphasize the need to demonstrate dissemination of lesions in space and time, and to exclude alternative diagnoses[8,12]. Contrast enhanced MRI is the only method to assess acute disease and acute inflammation[8] but increasing concerns regarding potential long-term gadolinium brain deposition could potentially restrict contrast application as an important diagnostic tool[13-17]. Additionally, the differentiation of MS lesions from brain white matter lesions of other origins can sometimes be challenging due to their resembling morphology at lower magnetic field strengths.

While MRI is certainly the best diagnostic tool for MS patients, MR examinations and protocols should follow guidelines of the Magnetic Resonance Imaging in MS group (MAGNIMS) in Europe[18,19] or the Consortium of Multiple Sclerosis Centers (CMSC) in North America[20] for the diagnosis, prognosis and monitoring of MS patients. Standardized quality control studies in accordance with the latest guidelines across different hospitals and countries are also crucial[21].

MRI protocols tailored for MS diagnosis and disease progression monitoring comprise multiple MRI contrasts including contrast governed by the longitudinal relaxation time T_1, the spin-spin relaxation time T_2, the effective spin-spin relaxation time T_2*, and diffusion weighted imaging (DWI)[22]. Harmonization initiatives provided consensus reports for MRI in MS to move towards standardized protocols that facilitate clinical translation and comparison of data across sites[23-25]. T_2-weighted imaging is well established and frequently used in clinical practice for identification of white matter (WM) lesions, which are characterized by hyperintense appearance[26,27]. While being an important diagnostic criterion for MS[28], the WM lesion load correlates only weakly with clinical disability, due to its lack of specificity for lesion severity and the underlying pathophysiology[26,27,29]. This observation has triggered explorations into parametric mapping of the transverse relaxation time T_2 [30]. T_2*-weighted imaging has become increasingly important in imaging MS. The central vein sign in T_2* weighted MRI is considered to be a specific imaging marker for MS lesions[27,31-33]. T_2* is sensitive to iron deposition[34,35], which may relate to disease duration, activity and severity[36-

[38]. T_2* was also reported to reflect brain tissue changes in patients with minor deficits and early MS, and thus may become a tool to assess the development of MS already at an early stage[39,40].

Improvements in MRI technology promise to better identify changes in the CNS of MS patients and to provide clinicians with a better guide to enhance the accuracy and speed of an MS diagnosis[11]. Ultrahigh field (UHF, $B_0 \geq 7.0$ T) MRI benefits from an increase in signal-to-noise ratio (SNR) that can be invested in enhanced spatial or temporal resolutions, both key to superior imaging for more accurate and definitive diagnoses[41,42]. Transmission field (B_1^+) inhomogeneities that are an adverse attribute of the ^{1}H radio-frequency used at ultrahigh magnetic fields[43] would benefit from multichannel transmission using parallel transmit (pTx) RF coils and RF pulse design approaches that enhance B_1^+ homogeneity and thus facilitate uniform coverage of the brain[44].

With the advent of 7.0 T MRI, we have achieved more insight into demyelinating diseases such as MS with respect to increased sensitivity and specificity of lesion detection, central vein sign identification, leptomeningeal enhancement, and even with respect to metabolic changes[45]. MS lesions have long been shown from histopathological studies to form around veins and venules[46]. The perivenous distribution of lesions (central vein sign) can be identified with T_2* weighted MRI[46-48] at 3.0 T or 1.5 T, but can be best identified with UHF-MRI at 7.0 T[49-52]. Other than the central vein sign, UHF-MRI at 7.0 T has improved or uncovered MS-specific markers such as hypointense rim structures and differentiation of MS grey matter lesions[53-56]. A better delineation of these markers with UHF-MRI promises to overcome some of the challenges of differentiating MS lesions from those occurring in other neuroinflammatory conditions such as Susac syndrome[53] and neuromyelitis optica[54], while also identifying common pathogenetic mechanisms in other conditions or variants of MS such as Baló's concentric sclerosis[57,58].

Recognizing the challenges and opportunities of UHF-MRI for the detection and differentiation of MS lesions, this article describes our current technical approach to study cerebral white and grey matter lesions in MS patients at 7.0 T using different imaging techniques. The up-to-date protocol includes the preparation of the MR setup including the radiofrequency (RF) coils tailored to the UHF-MR, standardized screening, safety and interview procedures with MS patients, patient positioning in the MR scanner and acquisition of brain scans dedicated to MS. The article is meant to guide imaging experts, basic researchers, clinical scientists, translational researchers, and technologists with all levels of experience and expertise ranging from trainees to advanced users and applications experts into the field of UHF-MRI in MS patients, with the ultimate goal of synergistically connecting technology development and clinical application across disciplinary domains.

PROTOCOL

This protocol is for studies that are approved by the ethics committee of the Charité – Universitätsmedizin Berlin (approval number: EA1/222/17, 2018/01/08) and the Data Protection Division and Corporate Governance of the Charité – Universitätsmedizin Berlin. Informed consent has been obtained from all subjects prior of being included in the study.

1. Subjects

NOTE: Recruitment of MS patients usually takes place at few days up to some weeks prior to the MR investigations at 7.0 T.

1.1. Recruit MS patients by neurologists from the outpatient clinic on the basis of inclusion criteria (depending on the neuroimmunological question) and exclusion criteria (including for example implantable medical devices such as insulin pumps or pacemakers or pregnancy).

1.2. During the outpatient visit, give MS patients a short summary of the MR investigation at 7.0 T as well as an explanation of safety measures associated with a 7.0 T MR examination.

1.2.1 While precautionary measures, particularly at 7.0 T, should be taken and a list of contraindications (e.g., **Table 1**) should be made available to all, keep well-informed on new insights into safety considerations and decision-making processes, particularly with the wide range of available implants, from reliable literature sources[59-63]. The International Society for Magnetic Resonance in Medicine (ISMRM) and the Society for MR Radiographers, Technologists (SMRT) provide safety guidance regarding MR safety strategies and standards for implants and devices [64].

1.2.2 Together with the health, safety officer and medical staff, be well-informed of possible dangers, precautions and solutions that are available. The type of local RF coil used for examination is a key factor, as well as the position and type of the implant[59].

1.2.3 Make a risk/benefit assessment that conforms to local ethical considerations[63] in subjects with implants, devices, or tattoos and consider the gains lost when restrictions are too conservative.

1.3. Provide subjects with an appointment for the examination at the 7.0 T MR scanner one week ahead of the MR investigations. Contact patients with mobility problems or those visiting from another city earlier than this. In parallel to the appointment allocation, give subjects important information via electronic mail: this includes informed consent documents and forms as well as safety information including a list of contraindications (**Table 1**). This serves as preparation to the discussion covered in steps 1.9 to 1.14.

1.4. Once admitting the subject into the UHF-MR building or unit and confirming identification, assess their awareness about the potential dangers related to the UHF magnetic fields. Particular attention is necessary in cases of passively conducting implants and for implantable medical devices (e.g., pacemakers and insulin pumps).

1.5. Request that each subject fills a confirmatory form with regards to the safety requirements to enter the 5 Gauss (0.5 mT) zone, which is considered to be the 'safe' level of static magnetic field exposure for the general public. This safety zone around the perimeter of the main magnet of the MR scanner is specified by the distance at which the stray magnetic field is equivalent to 5 Gauss. The 5 Gauss line is commonly highlighted on the floor. Because of the long range of the magnetic stray field of a passively shielded 7.0 T MR scanner in our

case, use the external walls of the building to specify the safety zone instead of the 5 Gauss line.

NOTE: At the time when this recording was made, the world was undergoing the 2020 coronavirus pandemic and each subject needed to follow the corresponding guidelines that included the distancing rule of 1.5 m, mouth and nose protection as well as hand disinfection.

1.6. Inform subjects about the availability of lockers close to the entrance of the MR building, where they can safely stack away their valuables. Inform subjects that some of their personal belongings (mechanical watches, bank cards with magnetic stripes) constitute a potential safety hazard and/or might get damaged when close to the magnets after a certain period.

1.7. Accompany the subject to the preparation room where the subject will be examined by the physician, neurologist or study nurse.

1.8. Query on health status and intake of medications. Document within the case report form (CRF).

1.9. Before all investigative measures, query about potential MRI contraindications (pregnancy, all potential previous surgeries with potential foreign bodies, previous injuries with metallic objects, piercings, tattoos, hearing aids, claustrophobia, musculoskeletal problems, passively or actively conducting implants including dental implants, medical devices such as pace makers and insulin pumps).

1.10. Discuss details about the background and goals of the study *(information sent ahead via email)*. If relevant, give information regarding study sources (e.g., whether the study is investigator-initiated, industry-initiated or industry-sponsored). State institutional links and potential conflicts of interest. The subject must be able to comprehend the purpose of the study and its implications. The subject has the right to get access to their own data, if requested. One year following completion of the study, a report or publication will be freely available.

1.11. Discuss data protection and insurance-related information. All data undergoes pseudonymization before the start of the study. Record personal subject data (including name, date of birth, addresses, contact numbers and pseudonymization ID) in an identification list within the investigator site file (ISF) and lock up in a dedicated cabinet.

1.11.1 Retain data for a maximum period of 10 years. Only authorized people defined in the ethics approval of the study have password protected access to the data. Insurance-related information includes arrangements for the treatment and/or compensation in case of damage because of participation in the study. This information is sent ahead via email.

1.12. Outline the study's medical parameter measurements (e.g., blood pressure, heartrate, body weight, body height, body temperature, pregnancy test in the case of childbearing female subjects). *This information is also sent ahead via email.*

1.13. Outline the MRI examination. Inform each subject about potential benefits but also potential risks of undergoing an MRI examination at UHF magnetic field before entering the MRI safety zone. *This information is also sent ahead via email.*

1.14. Ensure ethical integrity, attest that the study has been approved by the ethics committee and reassure patients with respect to study participation. Inform the subject that participating in the examination is voluntary and that they may always abort the examination at any time, with no extra justification or negative consequences.

1.15. Obtain informed consent, oral as well as in writing.

1.16. Following consent, the subject will be allocated a pseudonymized ID and all data will be recorded and stored under this pseudonym.

2. MR setup preparation

NOTE: The following is performed before the subject arrives at the UHF-MR Building.

2.1. Switch on the MR acquisition software. The magnet is always on.

2.1.1 For some scanners (e.g., the Siemens MR system used to acquire the representative results in this protocol) a switch box in the operator room (**Figure 1**) initiates the MR system (gradients and software): Turn the key clockwise, press the blue **System on** button to start the software (syngo). A window appears on the scanner PC requiring password confirmation.

2.2. Connect an RF coil dedicated to head MRI to the MR system. On a Siemens 7.0 T, this is typically a 1-channel circular polarized (CP) transmit (1Tx (CP)), 24-channel receive (24Rx) RF coil (**Figure 2**) or alternatively a 1Tx(CP)/32Rx RF coil. These RF coils are connected via 4 plugs to the patient table (labelled X1 – X4).

NOTE: On a Philips or General Electric (GE) 7.0 T MR system, a typical head coil would be a 2Tx(CP)/32Rx RF coil. This RF coil is connected via 3 plugs and interface boxes to the patient table. All these RF coils do not require patient specific tuning and matching.

2.3. For small RF coils, use earplugs instead of headphones as hearing protection.

2.4. Prepare the patient bed. Have earplugs, soft pillows, leg cushion, blanket and bed cover sheet readily available, in the vicinity of the MR scanner.

2.5. Patient bed should be in the retractable position ready for the subject.

3. Subject preparation

3.1. Guide the subject to the locker room and ask the subject to change into scrubs. Only underwear free of metal and free of radiofrequency identification chips must be worn. Ensure once again that all metallic objects such as glasses, jewellery, mobile phones do not enter the 7.0 T MR operator and scanner room.

3.2. Carry out all preparatory measures mentioned in step 1.11.

3.3. Ask subjects to empty their bladder prior to the MR measurements. Perform pregnancy tests in female subjects of child-bearing age.

3.4. Accompany the volunteer to the 7.0 T MR scanner room via the operator room. Before entering the 7.0 T MR scanner room, ensure once again that no metallic objects are present.

3.5. Walk slowly to the 7.0 T examination table. Passively shielded magnets have a larger size of the magnetic fringe field than actively shielded ones. Small ferrous objects could already experience attractive forces/torques at the door of the room containing a passively shielded magnet.

3.6. Ask the subject to lie down on the table and make them as comfortable as possible. Offer small head and arm comfort pillows as well as leg cushion as well as a blanket to avoid the subject from getting cold.

3.7. Connect an MRI-safe pulse oximeter to the subject to monitor oxygen saturation (SpO_2), heart rate readings and vital signs from the subject during the MRI procedure.

3.8. Provide earplugs and a hand-held squeeze ball (alarm) to be used during the MR examination in case of an emergency. Ask the subject to press the squeeze ball to confirm that it is functioning properly.

3.9. Instruct the subject to move closer to the RF head coil (**Figure 2**). Shift the TX-Part and upper RX-coil part of the RF coil towards the service end for positioning the head of the subject (**Figure 2**). Switch on the isocentre positioning device.

3.9.1 In some MR scanners (e.g., Siemens and GE MR systems), use a laser. Move the subject table very slowly so that the laser positioning is in full alignment with the marker cross on top of the RF coil. Save this position. During the laser positioning, ask the subject to close their eyes. Other UHF-MR vendors have other systems for positioning. In all cases, make sure that the mark on the RF coil is aligned to the isocentre positioning device.

3.10. Make sure that the head is positioned carefully and ascertain that the subject is comfortable.

3.11. Move the subject table very slowly to the isocenter of the MR scanner. At 7.0 T, it is particularly important to move the table slowly to avoid and reduce side effects such as metallic taste, vertigo, dizziness that are caused by induction currents[65-67]. To meet this requirement, adjust the speed profile of the table motion to B_0*(grad(B_0)) by some vendors. It is recommended that the patient table motion be set lower than 0.66 T/s [67].

3.12. Communicate with the subject while driving the table and explain that any potential side effects will disappear as soon as the table comes to a halt. The subject might still feel

dizzy or experience a metallic taste when moving the table towards the center of the magnet. In our experience, these effects are minor and completely reversible[67,68].

3.13. Before leaving the scanner room, ensure that the subject is comfortable and willing to start with the MR examination.

3.14. Use the intercom to check proper communication with the subject after leaving the scanner room. The subject can contact the study personnel at any time.

3.15. Continue monitoring the subject's condition and verify whether the subject is still comfortable throughout the entire examination, including all the next steps till the end of the study.

4. Data acquisition

NOTE: In the following, some of the references to user interface actions or specific scan procedures may only be valid for one specific MR system (7.0T Magnetom, Siemens healthineers, Erlangen, Germany). The commands and procedures vary between vendors and software versions. The following protocol follows the guidelines of the Magnetic Resonance Imaging in MS group (MAGNIMS) in Europe[18,19] and the Consortium of Multiple Sclerosis Centers (CMSC) in North America[20] for the diagnosis, prognosis and monitoring of MS patients.

4.1. Enter the required study and subject details (project number, pseudonymized ID, date of birth, height, weight, subject position (i.e., headfirst and supine position), name of investigator). The steps vary between 7.0 T MR systems from different vendors. In all cases, make sure the correct study protocol is loaded.

4.1.1 For Siemens scanners, click on the upper bar of the display (**Patient | Registration**) in the syngo software. Type in patient information, select study protocol and click on **Exam**. The selected study protocol is loaded, and the examination window opens. On the right side of this window any saved imaging sequences for the selected study protocol will appear.

4.2. Run imaging sequences in the order given within the selected study protocol. The parameters for these imaging sequences should be planned ahead of patient investigations and saved according to the above CMSC and MAGNIMS guidelines for the diagnosis[18] as well as prognosis and monitoring of MS patients[19].

4.3. Adjustments and scout images

4.3.1 Prior to data acquisition of the MS examination, perform the necessary adjustments using the **Localizer** sequence (also referred to as scout sequence). This is usually a gradient echo (GRE) sequence and contains the adjustment protocols that need to be carried out before scanning.

NOTE: Adjustments include a correction (shimming) of the inhomogeneous static magnetic (B_0) field. B_0 inhomogeneities occur because of the large magnet and due to susceptibilities within the body (e.g., air, bone, blood) and their distribution. Inhomogeneities broaden the frequency distribution of the spins and can also cause significant intravoxel dephasing; this is not an issue in RF-refocused (spin-echo) sequences but can reduce signal amplitude considerably in most of the following sequences, particularly the T_2^*-weighted acquisitions. Adjustments are automatically done on clinical MR scanners (devices with field strengths $B_0 \leq 7.0$ T). On some scanners (e.g., Siemens 7.0 T MR scanners) adjustments are usually actively started by the operator. For specific detail on how to select and operate sequences refer to the operator manual specific to the system configuration.

4.3.2 Select the **Localizer**. On Siemens scanners, mark the sequence on the right-hand side of the window and click on the left arrow to move the sequence to the left side of the window to queue it within the workflow. Make sure that all channels are selected for the RF coil used. The **Localizer** sequence is also important for planning the orientation of the imaging slices in the subsequent sequences. At this point no image is available, so the adjustment volume cannot be altered.

4.3.3 Run adjustments as required for the specific MR system (refer to the operator manual). On Siemens scanners, this includes frequency and transmitter adjustments to set the basic frequency and the voltage required for the RF coil and amplifier power used, as well as 3D shimming to correct the inhomogeneity of the static magnetic field (**Figure 3**):

4.3.4 Choose **Options | Adjustments**. Tabs for Frequency, Transmitter, 3D Shim and others will appear in the lower bar of the window. Under **Frequency**, select **Go** until the basic frequency is centred and Yes appears. Under **Transmitter**, set the voltage according to the RF coil and amplifier power used (for the 24-channel receive Rx RF head coil we employ 300 V) and **Apply**.

4.3.5 Under 3D Shim, select **Measure** and when the B_0 Map is generated, press **Calculate** to acquire the shim values. Repeat **Frequency** and **3D Shim** adjustments at least twice until the shim values are consistent with the previous. Press **Apply** and **Close**. On Philips and GE 7.0 T scanners, carry out adjustments in the background prior to each sequence (feedback is required from the operator for adjustment control).

4.3.6 Run the **Localizer** sequence in 3 orientations. Sequence parameters: Acquisition time (TA) = 160 ms. Since no image is yet available, set the position at isocenter, rotation = 0 °. Other parameters: matrix = 256×256, FOV = 250 mm, slice thickness = 7.0 mm, slice gap = 7.0 mm (100 %), TR = 7.0 ms, TE = 3.03 ms, Averages (avg) = 1, Flip angle (FA) = 2 °, no fat or water suppression. *Slice group 1* (sagittal orientation, phase encoding direction A>P), *Slice group 2* (transversal orientation, phase encoding (PE) direction A>P), *Slice group 3* (coronal orientation, phase encoding direction R>L). Three slices are acquired for all slice groups. At this point no changes are made to the geometry.

4.3.7 Acquire the scout images.

4.3.8 Confirm whether the adjustment volume was set correctly using the **Localizer** MR images. Align the adjustment volume with the FOV and centrally aligned with the subject's head. If not aligned, align correctly and perform the adjustments again.

4.3.9 Important: Each time the adjustment volume or the number of RF channels used is changed, carry out adjustments again.

4.3.9.1 On Siemens systems, avoid this by copying the adjustment volume from the last **Localizer** where the adjustment volume was correctly set: Select the last scan with the correct adjustment, right click **Copy Parameter**, and select **Adjust Volume** in the open window. Circumstances where further adjustments are required include special imaging sequences that require more intensive shimming techniques (e.g., echo planar imaging (EPI)).

4.4. Acquisition of dedicated MR imaging sequences

4.4.1 Several sequences with different contrasts (T_1, T_2, T_2*, phase, QSM, diffusion) exist for studying MS pathology (**Figure 11**). Those best suited for the clinical needs or research questions may be selected and organized within study protocols on the MR system for use during the specific relevant research projects or clinical studies. Several practical guides and reviews exist for studying, detecting and defining multiple sclerosis lesions on MRI [8,50,69]. Each MR system will have different operational procedures and user interface for acquiring the dedicated MR sequences (**Figure 4**). On Siemens systems, view the list of MR methods (sequences) on the right for each study protocol and queue in the sequence list of the examination window (on the left). Below are some sequences that we employ on a Siemens 7.0 T MR scanner to study MS pathology. When planning sequence positionings, make sure to repeat adjustments if that is required.

4.5. Magnetization Prepared - RApid Acquisition Gradient Echo (MPRAGE)

4.5.1 MPRAGE is a T_1-weighted 3D sagittal inversion recovery-prepared spoiled-GRE sequence for high spatial resolution and T_1-contrast. Its purpose is typically anatomical, and it is useful to assess volume loss in MS[70]. It was first applied in MS patients to improve the detection of contrast-enhanced lesions (CELs)[71]. MPRAGE provides excellent T_1-dependent contrast between gray matter (GM), white matter (WM), and cerebrospinal fluid (CSF) even without contrast agent[72]. In combination with a T_2-weighted sequence such as FLAIR (see below), it is a widely used T_1-weighted technique in multimodal segmentation approaches and voxel-based morphometry[73]. Cortical MS lesion detection and classification using MPRAGE is considerably improved by the better parallel imaging performance and increasing SNR and spatial resolution available at 7.0 T [74].

4.5.2 Use the following MPRAGE sequence parameters: TA = 5 min 3 s, 3D mode, isotropic resolution = [1.0×1.0×1.0]mm³, matrix = 256×256×256, FOV = 256 mm, sagittal orientation, PE direction A>P, slices per slab = 192, slice thickness = 1.0 mm, slice gap = 0.5 mm, TR = 2300 ms, TE = 2.98 ms, avg = 1, concatenations = 1, no filter, inversion recovery evolution time TI = 900 ms, FA = 5 °, no fat or water suppression, base resolution = 256, parallel imaging with GRAPPA, AF_{PE} = 2 (**Figure 4A**).

4.5.3 Acquire in sagittal orientation which is in alignment with the interhemispheric fissure. Since MPRAGE is a 3D sequence, the images can still be registered onto the baseline scan at the end of the study.

4.6. Magnetization-Prepared 2 – Rapid Acquisition Gradient Echo (MP2RAGE)

4.6.1 This is a T_1-weighted 3D sequence with simultaneous T_1 mapping; a two inversion-contrast magnetization-prepared rapid gradient echo sequence for robust white matter lesion volume measurements[75]. The MP2RAGE sequence produces images with different contrasts e.g., two gradient echo images with different inversion times and flip angles, a T_1w image without a noisy background and a T_1 map. Quantitative T_1 mapping provides further diagnostic information in MS patients to better discriminate lesion subtypes and enable faster staging of disease activity[76]. MP2RAGE was recently shown to improve the visualization of subpial intracortical lesions (**Figure 13A**)[77], which are associated with meningeal inflammation in MS[78] and are largely difficult to detect even with higher field strengths and advanced methods. The open-source MP2RAGE code is available from the developer: https://github.com/JosePMarques/MP2RAGE-related-scripts

4.6.2 Use the following MP2RAGE sequence parameters: TA = 11 min 37 s, 3D dimension, sagittal orientation, PE direction A>P, spatial resolution = [1.0×1.0]mm², matrix = 256×256, FOV = 256 mm, FOV phase = 93.75 %, slabs = 1, slices per slab = 176, slice thickness = 1.0 mm, slice gap = 0.5 mm, TR = 5000 ms, TE = 3.18 ms, avg = 1, concatenations = 1, TI 1 = 700 ms, TI 2 = 2500 ms, FA 1 = 4 °, FA 2 = 5°, no fat or water suppression, base resolution = 320, parallel imaging with GRAPPA, AF_{PE} = 3 (**Figure 5**).

4.6.3 Run the MP2RAGE with the same orientation and positioning as the MPRAGE.

4.7. Fluid-Attenuated Inversion Recovery (FLAIR)

4.7.1 FLAIR is a 3D sequence that uses T_2-weighted fluid-attenuated inversion recovery (FLAIR) with CSF signal suppression to assess dissemination of new MS lesions over time (*on Siemens scanners it is used in conjunction with SPACE (Sampling Perfection with Application-optimized Contrasts using different flip angle Evolutions, imaging module*). Advantages of this sequence include high isotropic resolution, low SAR, parallel imaging possibility, CSF suppression and therefore better detection of lesions at brain parenchymal boundaries. FLAIR is particularly beneficial to identify cortical lesions (**Figure 13B**)[79] and leptomeningeal enhancements (LME) postcontrast in MS brains[80]. Interestingly, detection of LME in MS patients at 1.5 T was significantly higher when using FLAIR CUBE (imaging module for GE MR systems) compared to FLAIR SPACE (Siemens)[81]. 3D FLAIR SPACE was shown to be an attractive T_2-weighted sequence complementing the above T_1-weighted MP2RAGE sequence for lesion detection in MS patients[76]. Typically, both sequences are co-registered with cross-sectional lesion segmentations to render joint MS lesion maps[82]. Recently FLAIR (on a 3.0 T Philips MR system) identified that Susac syndrome patients were significantly more likely to present with LME than MS patients[83].

4.7.2 Use the following FLAIR sequence parameters: TA = 6 min 16 s, 3D model, sagittal orientation, PE direction A>P, isotropic resolution = [0.8×0.8×0.8]mm³,

matrix = 320×320×320, FOV = 256 mm, slabs = 1, slice oversampling = 18.2 %, slices per slab = 176, FOV phase = 87.5 %, slice thickness = 0.80 mm, TR = 8000 ms, TE = 398 ms, avg = 1, concatenations = 1, raw and image filter, TI = 2150 ms, no fat or water suppression, acceleration factor along the phase encoding direction AF_{PE} = 4 (**Figure 6**).

4.7.3 Run the sequence in sagittal orientation, same as the MPRAGE and MP2RAGE sequences.

4.7.4 Increase the FOV phase in the sequence parameter map to 100% if the nose is outside the yellow frame. This changes the TA to 6 min 56 s.

4.8. Multi-Echo Fast Low-Angle Shot (FLASH-ME)

4.8.1 FLASH-ME is a 2D T_2*-weighted GRE sequence acquiring multiple echoes with different echo times. A similar sequence was used previously at 7.0 T as a quantitative tool for estimating T_2* relaxation rates, to study patterns of cytoarchitectural organization throughout the entire cortex in health controls [84]. More recently, quantitative T2* mapping was used to study cortical tissue integrity in MS patients, and cognitive impairment was shown to correlate with T2* increase, independent from cortical thickness or presence of lesions[85]. When using the longest echo time only, the sequence is used to delineate MS white matter lesions that are centred around a small venous vessel (central vein sign, **Figure 12**), especially those close to the ventricles (**Figure 14a**)[42,55].

4.8.2 Use the following FLASH-ME sequence parameters: TA = 12 min 10 s, 2D mode, transversal orientation, in plane resolution = [0.47×0.47]mm², matrix = 512×512, FOV = 238 mm, slices = 52, slice thickness = 2.0 mm, no slice gap, PE direction R>L, TR = 1820 ms, TE_{1-8} = 4.08 ms, 7.14 ms, 10.20 ms, 13.26 ms, 16.32 ms, 19.37 ms, 22.43 ms, 25.49 ms (make sure that the increment in the echo time is a multiple of the fat-water shift of 3.5 ppm), avg = 1, concatenations = 1, FA = 35 °, no fat suppression (**Figure 7**).

4.8.3 Use the **3D MPRAGE** and the coronal, transversal **Localizer** images to plan the geometry of the 2D FLASH-ME scan.

4.8.4 Adjust the FOV and slices such that the entire head is in the middle (see above).

4.8.5 Move and tilt the 2D FLASH-ME FOV, using the zoom and panning tool on the sagittal MPRAGE images such that the lower boundary of the FOV (yellow frame) is in line with the lower corpus callosum line (**subcallosal plane**).

4.8.6 Move the entire stack after angulation, such that the uppermost layer ends with the skull calotte. The stack does not cover the entire brain. Larger stacks increase measurement time and introduce nasal-aural cavity magnetic susceptibility artifacts.

4.8.7 Modify the adjustment volume if it is no longer aligned with the geometry volume. If required repeat the adjustments (see above).

4.9. Susceptibility Weighted Imaging (SWI)

4.9.1 For SWI, use magnitude and phase data of a fully flow-compensated 3D T_2^*-weighted GRE sequence. To enhance susceptibility contrast, weighting masks are generated from phase data and multiplied with magnitude images in SWI[86]. SWI enhances the contrast between veins and surrounding tissue[87], and also identifies iron deposition in MS patients[88]. A deposition of iron-laden macrophages occurs at the edges of chronic demyelinated MS lesions[89], and this presents as a hyperintense signal at the lesion border on phase images[89,90] and a decreased signal (hypointense rim) on T_2^*-weighted images post-processed using SWI in vivo and post mortem[91] (**Figure 14b**). 3D encoding enables shorter TRs and lower flip angles, thereby enabling whole brain coverage, reducing acquisition time and lowering sensitivity to B_1^+ field perturbations[92]. Parallel imaging also reduces acquisition time; generalized autocalibrating partially parallel acquisition (GRAPPA) parallel imaging reconstructs magnitude and phase images for each channel and combines them to generate the final images[93,94].

4.9.2 Use the following SWI sequence parameters: TA = 9 min 26 s, 2D mode, spatial resolution: [0.3×0.3]mm², matrix = 768×768, FOV read = 256 mm, FOV phase = 68.75 %, slabs = 1, slices per slab = 120, slice thickness = 1.0 mm, slice gap = 0.2 mm, strong transversal orientation, PE direction R>L, TR = 30 ms, TE = 15.3 ms, avg = 1, concatenations = 1, FA = 30 °, no fat or water suppression, base resolution = 768, phase resolution = 100 %, slice resolution = 100 %, phase partial Fourier = 6/8, slice partial Fourier = 6/8, parallel imaging with GRAPPA, AFPE = 2 (Figure 8).

4.9.3 Acquire in transversal orientation and ***do not*** introduce any angulation as this makes postprocessing more difficult.

4.9.4 Shift the slice slab in the cranial direction so that the uppermost border is aligned with the skull calotte. Displace the slab in ventral or dorsal direction, so that the brain is completely in the middle of FOV.

4.10. Quantitative Susceptibility Mapping (QSM)

4.10.1 For QSM, use a 2D T_2*-weighted GRE sequence (employing six echo times with flow compensation for the first echo). QSM is a successor to SWI and the idea behind it is to provide a voxel-by- voxel estimate of the susceptibility distribution[95]. QSM makes use of phase images and generates a 3D susceptibility distribution. The voxel intensity is linearly proportional to the apparent magnetic susceptibility of the underlying tissue. When studying MS pathology, QSM provides important information about tissue composition and microstructure such as myelin content in white matter and iron deposition in gray matter[95]. The different MS pathophysiological processes that contribute to MR-measurable signal changes are complex, such that a combination of different MR methods is beneficial: while QSM is more sensitive to MS-related tissue changes, it also shows an additive effect of iron accumulation and demyelination (both promote magnetic susceptibility), this is in contrast to T_2* mapping, in which both pathophysiologic processes in MS will exert opposing effects: demyelination increases T_2* rate while iron deposition decreases T_2*[96]. QSM accurately resolves the magnetic susceptibility spatial pattern compared to phase images and hence depicts both solid and rim patterns of susceptibility more precisely and reliably[97]. By combining T2*-

weighted images with SWI and QSM, it is also possible to study changes in iron-content in lesions during disease progression in MS: while non-iron-laden lesions are hyperintense in all sequences, iron-laden lesions are hypointense in T2* and SWI but not QSM [98].

4.10.2 Use the following QSM sequence parameters: TA = 7 min 43 s, 2D mode, slabs = 1, PE direction A>P, in plane resolution = [0.49×0.49]mm², matrix = 448×448, FOV read = 220 mm, FOV phase = 90.6 %, slices per slab = 96, slice thickness = 1.0 mm, slice oversampling = 8.3 %, TR = 36 ms, TE_{1-6} = 6.15 ms, 11.22 ms, 16.32 ms, 21.42 ms, 26.52 ms, 31.62 ms, avg = 1, concatenations = 1, image filter, FA = 30 °, no fat or water suppression, base resolution = 448, phase partial Fourier = 6/8, slice partial Fourier = 6/8, parallel imaging with GRAPPA, AF_{PE} = 2 (**Figure 9**).

4.10.3 Move and tilt the FOV, using the zoom and panning tool on the sagittal MPRAGE images such that the lower boundary of the FOV (yellow frame) is in line with the lower corpus callosum line (**subcallosal plane**).

4.10.4 Move the slice stack cranially so that the top layer is aligned with the skull calotte.

4.11. Diffusion-weighted Echo-Planar Imaging (DW-EPI)

4.11.1 For DW imaging, use a **2D EPI** sequence with 64 different diffusion encoding directions at b-value b = 0 s/mm² and b = 1000 s/mm². DW imaging detects discreet changes in tissue microstructure, including diffuse neurodegeneration and demyelination in NAWM in early stage MS that is often missed on conventional MRI[99,100]. Previous diffusion studies in MS reported increased mean diffusivity in cortical lesions[101]. A more recent study at 7.0 T revealed similar findings but also a lower intracellular volume fraction in early stage MS; the intracellular compartment was separated from the isotropic volume fraction (oedema or CSF) and extracellular space by fitting a three-compartment tissue model to the DW images [102]. A reduction in intracellular volume fraction was not only reported in cortical and WM lesions but also in the NAWM, when compared to WM of controls[102]. In WM lesions, the reduced intracellular compartment was accompanied by increased mean diffusivity and fractional anisotropy, indicating demyelination and axonal loss[102]. DW-EPI is commonly associated with geometric distortions that appear as stretched or compressed pixels in the acquired image. In order to compensate for this, reversed phase gradient approaches have been introduced, in which the same slice is acquired twice using opposite phase encoding (PE) polarities [103,104]. The opposite spatial distortion patterns can be aligned, and the images combined using registration tools. For distortion correction, the same image is acquired with a reversed PE direction but without diffusion weighting, hence a reduction in acquisition time.

4.11.2 Use the following DW-EPI sequence parameters: TA = 14 min 02 s, 2D dimension, transversal orientation, A>P PE direction, spatial resolution = [1.95×1.95]mm², matrix = 256×256, FOV read = 500 mm, slices = 30, FOV phase = 100.0 %, slice thickness = 2.0 mm, slice gap = 2.0 mm, TR = 12000 ms, TE = 115 ms, avg = 1, concatenations = 1, fat suppression, base resolution = 256, phase resolution = 100 %, phase partial Fourier = 6/8, parallel imaging with GRAPPA, AF_{PE} = 3, diffusion mode = MDDW, 2 diffusion weightings: b-value 1 = 0 s/mm², b-value 2 = 1000 s/mm², diffusion directions = 64 (**Figure 10**).

4.11.3 Acquire in transversal orientation and ***do not*** introduce any angulation as this makes postprocessing more difficult.

4.11.4 Move the FOV so that the upper line of the layer block is aligned with the skull calotte. Shift dorsoventrally so that the brain is exactly in the middle of the FOV.

4.11.5 Acquire the sequence in two reversed polarities of the phase-encoding (PE) direction to cancel distortion artefacts during post processing. To run the reversed polarity sequence, repeat the 2D EPI sequence again, now selecting the version of the sequence with the PE direction in P>A. *Changed Sequence parameters*: TA = 1 min 14 s, P>A PE direction, 1 diffusion weighting: b-value = 0 s/mm².

4.11.6 Run this sequence with the same orientation and positioning as the previous 2D EPI sequence.

4.11.7 Confirm that the phase encoding direction is set to P>A in the parameter tab *Routine*. If not, change by inputting 180°.

4.11.8 As soon as the last sequence is finished and reconstructed, the MRI examination is ready.

4.11.9 Document all acquired sequences and their associated descriptions in the CRF.

5. Concluding the MR examination

5.1. Enter the MR scanner room and move the subject table slowly away from the isocenter.

5.2. Assess the condition of the subject and query about any possible side effects before, during or after the measurements. Query specifically about dizziness, light flashes, feeling of heat or cold, general discomfort, muscle twitching, metallic taste, or any other effects.

5.3. Document all observations (including side effects) in the CRF.

5.4. Following a final consultation, the subject is accompanied to the changing room, then to the locker to pick-up the valuables stored there and then to the exit of the building. As safety measure always accompany visiting subjects.

5.5. File all written documents (CRF, subject ID list, study consent forms) in the investigator site folder and lock in a safe place. The storage period is at least 10 years.

6. Data backup

NOTE: Each MR center follows its own guidelines to save and safely backup MR data. Digital MR data should be stored on a password-protected server. The procedure below is typical for a Siemens 7.0 T MR system.

6.1. Select the participant ID number in the **Patient Browser** and select **Transfer**.

6.2. Select **Export to Off-line** and enter the path of a local folder (e.g., C:\temp).

6.3. Check if the process is finished (from **Transfer | Local Job Status**).

6.4. Select Advanced User (**Ctrl+Esc**) and unlock by entering administrative password.

6.5. Once Advanced User is enabled, go to Windows Explorer (**Ctrl+Esc**).

6.6. Move the Dicom data from local folder to a secure Dicom data study folder on the password-protected server.

7. System shutdown

7.1. Shut down the system according to the system's requirements. For Siemens scanners, use the upper bar in the syngo software to shut down the software. Switch off the MR system (blue button on Siemens scanners) only after the software has shut down. Turn the key to the left.

Representative Results

A 26-year-old woman diagnosed with relapsing remitting MS (RRMS) was examined at 7.0 T using the above protocols (**Figure 11**). Some distortions in the B_1^+ profile can be observed in the MR images. This is anticipated when moving to higher resonance frequencies[43]; the shorter wavelengths increase destructive and constructive interferences[105,106]. To acquire the MR images (**Figure 11-14**), we used a single channel transmit volume coil on a Siemens 7.0 T MR system in which a manual adjustment of phase and amplitude was not possible to offset the B_1^+ inhomogeneities. Multi-transmit technologies offer the degrees of freedom of parallel transmission required to dynamically modulate the B_1^+ field distribution[44]. While the B_1^+ pattern cannot be modified for a single transmit element of a given coil, the electromagnetic properties of the surrounding environment may be altered, as has been shown with dielectric padding filled with water[107] or calcium titanate suspensions[108] used at 7.0 T. Geometrically tailored dielectric pads have been shown to be effective at imaging the brain [109,110] and particularly the inner ear[111], a challenging place to image due to inhomogeneities from susceptibility differences between inner ear fluids and bone.

Shown in **Figure 11** are sagittal and transversal views of the patient's brain using different protocols providing different contrasts. Four and a half years prior to the 7.0 T MR examination the patient presented with diplopia and blurry vision. Diagnosis was initially established, based on the 2017 McDonald criteria[8] due to periventricular, juxtacortical and infratentorial MR lesion distribution and based on the occurrence of both gadolinium-enhancing and non-enhancing lesions at 3.0 T. CSF findings were within normal limits. Medication with natalizumab (NTZ) was subsequently initiated. The MS diagnosis was subsequently challenged due to an increase in T_2 lesions and multiple clinical relapses with incomplete remission despite the highly efficacious NTZ treatment. However, 7.0 T MRI supported the MS diagnosis by revealing the central vein sign in the majority of periventricular and juxtacortical lesions (**Figure 12**). The MS diagnosis was further corroborated by cortical

pathology (**Figure 13**) and hypointense rim structures surrounding a subset of T_2 hyperintense lesions (**Figure 14**). The diagnostic re-evaluation also included a search for other autoimmune, infectious, and metabolic disorders but did not reveal further abnormal results. Eventually the patient was tested positive for antibodies against NTZ, indicating antibody-mediated neutralization and explaining the insufficient treatment response towards NTZ [112]. Therefore, an MS diagnosis with an unresponsiveness towards NTZ therapy was concluded in this patient. Medication was switched from NTZ to Ocrelizumab and the patient has been relapse-free during the ensuing stages.

Figure 1. Switch box of Siemens MR scanner

Figure 2. Connecting a dedicated RF coil to the MR system. (**a**) Transmit (Tx), 24- or 32 channel receive (Rx) radio frequency head coil tailored for brain MRI at 7.0 T (**b**) Instruct the subject to move closer to the RF head coil and position the head of the subject over the lower RX-coil and beneath the upper RX-coil (left panel). Next move the TX-part of the RF head coil over the RX-coil (bottom right).

Figure 3. Running adjustments (Siemens system). (**a**) Basic frequency adjustment, (**b**) Transmitter voltage adjustment, (**c**) Generation of B_0 Map and 3D shimming.

Figure 4. MR sequence planning on 7.0 T MR systems from different vendors. (**a**) Siemens, (**b**) Philips and (**c**) General Electric.

Figure 5. Planning 3D MP2RAGE imaging sequence

Figure 6. Planning 3D SPACE-FLAIR imaging sequence

Figure 7. Planning 2D FLASH-ME imaging sequence

Figure 8. Planning 3D susceptibility weighted imaging sequence

Figure 9. Planning QSM-FC

Figure 10. Planning diffusion-weighted echo-planar imaging sequence

Figure 11. Representative results of high-resolution brain MRI of an RRMS patient Upper panel from left to right: (**a**) sagittal view of a T_1w 3D inversion recovery-prepared spoiled-GRE sequence (MPRAGE), (**b**) transversal view of T_1w 3D MPRAGE, (**c**) transversal view of T_2*w 2D FLASH sequence with multi-echo readout (FLASH-ME), (**d**) transversal view of a T_2w fluid-attenuated inversion recovery using sampling perfection with application-optimized contrasts using different flip angle evolutions (SPACE-FLAIR), (**e**) transversal view of flow compensated quantitative susceptibility mapping (QSM-FC). Lower panel from left to right: (**f**) sagittal view of a T_1w 3D magnetization-prepared rapid gradient echo sequence (MP2RAGE), (**g**) transversal view of T_1w 3D MP2RAGE, (**h**) transversal view of 3D susceptibility weighted imaging (SWI) using magnitude and phase data of a fully flow-compensated GE sequence, (**i**) combined fractional anisotropy map and directional map of an echo-planar diffusion-weighted imaging sequence (2D EPI), (**j**) transversal view of T_2*w 2D gradient echo imaging with flow compensation (GRE-FC).

Figure 12. Representative white-matter MS lesions with central vein sign (**a and b**) Transversal view of T_2*w 2D FLASH sequence with multi-echo readout (FLASH-ME) reveals highly MS-specific central vein sign (red arrow) within exemplary periventricular lesions, (**c**) a right-hemispheric thalamic lesion (**d**), and a parietal juxtacortical lesion, substantiating the patient's MS diagnosis.

Figure 13. Representative cortical MS lesion. (**a**) Sagittal view of a T_1w 3D magnetization-prepared rapid gradient echo sequence (MP2RAGE) delineates subpial cortical lesion (red arrow heads) within parietal cortex (**b**) with corresponding hyperintensity in transversal view of a T_2w fluid-attenuated inversion recovery (SPACE-FLAIR), indicating the occurrence of cortical MS pathology in the relapsing-remitting MS patient.

Figure 14. Representative hypointense rim structures. (**a**) Transversal view of T_2*w 2D FLASH sequence with multi-echo readout (FLASH-ME) reveals an ovoid periventricular MS lesion, and (**b**) transversal view of 3D susceptibility weighted imaging (SWI) delineates a hypointense rim structure around the lesion, suggesting iron-laden macrophages to be present as a potential surrogate for MS lesion activity.

Table 1. Principal contraindications of an MRI examination. The most common contraindications are metallic implants. Implants are becoming increasingly MR safe (MRI-conditional) but remain a major concern.

Discussion

The protocol presented here describes a series of MRI sequences with different contrasts that are typically used when examining MS patients at 7.0 T. Together with emerging technological developments, they provide the basis for explorations into more advanced applications in metabolic or functional imaging.

Aside from brain lesions, lesions in the spinal cord frequently affect MS patients causing motor, sensory and autonomic dysfunction. However spinal cord imaging, particularly at 7.0 T, is technically challenging[113]. Further developments in parallel transmission and parallel imaging are warranted to overcome the hurdles of distorted B_1 field profiles[114].

The goal of this protocol is to disseminate and synergistically connect technology developments and clinical application across disciplinary domains. Aside from the expected enhancements in spatial and temporal resolution, opportunities from the changing physical characteristics of higher magnetic fields include better contrasts in susceptibility-weighted imaging (SWI) and phase-contrast techniques[115], as well as imaging of X-nuclei such as sodium[116,117] and fluorine[118-120] for a more in depth assessment of the pathology as well as therapeutic monitoring.

Acknowledgements

This project (T.N.) has received funding in part from the European Research Council (ERC) under the European Union's Horizon 2020 research and innovation program under grant agreement No 743077 (ThermalMR). The authors wish to thank the teams at the Berlin Ultrahigh Field Facility (B.U.F.F.), Max Delbrueck Center for Molecular Medicine in the Helmholtz Association, Berlin, Germany; at the The Swedish National 7T Facility, Lund University Bioimaging Center, Lund University, Lund, Sweden and at the ECOTECH-COMPLEX, Maria Curie-Skłodowska University, Lublin, Poland for technical and other assistance.

Disclosures

There are no competing financial interests to be declared.

References

1 Filippi, M. et al. Multiple sclerosis. *Nature Reviews Disease Primers.* **4** (1), 43 (2018).

2 Krieger, S. C., Cook, K., De Nino, S., Fletcher, M. The topographical model of multiple sclerosis: A dynamic visualization of disease course. *Neurology: Neuroimmunology & Neuroinflammation.* **3** (5), e279 (2016).

3 Kutzelnigg, A. et al. Cortical demyelination and diffuse white matter injury in multiple sclerosis. *Brain.* **128** (11), 2705-2712 (2005).

4 Kuchling, J., Paul, F. Visualizing the Central Nervous System: Imaging Tools for Multiple Sclerosis and Neuromyelitis Optica Spectrum Disorders. *Frontiers in Neurology.* **11** 450 (2020).

5 Lassmann, H. Multiple Sclerosis Pathology. *Cold Spring Harbor Perspectives in Medicine.* **8** (3) (2018).

6 Miller, D. H., Chard, D. T., Ciccarelli, O. Clinically isolated syndromes. *The Lancet Neurology.* **11** (2), 157-169 (2012).

7 van der Vuurst de Vries, R. M. et al. Application of the 2017 Revised McDonald Criteria for Multiple Sclerosis to Patients With a Typical Clinically Isolated Syndrome. *JAMA Neurologyogy.* **75** (11), 1392-1398 (2018).

8 Thompson, A. J. et al. Diagnosis of multiple sclerosis: 2017 revisions of the McDonald criteria. *The Lancet Neurology.* **17** (2), 162-173 (2018).

9 Filippi, M., Preziosa, P., Rocca, M. A. Multiple sclerosis. *Handbook of Clinical Neurology.* **135**, 399-423 (2016).

10 Rovira, A., de Stefano, N. MRI monitoring of spinal cord changes in patients with multiple sclerosis. *Current Opinion in Neurology.* **29** (4), 445-452 (2016).

11 Filippi, M. et al. Assessment of lesions on magnetic resonance imaging in multiple sclerosis: practical guidelines. *Brain.* (2019).

12 Kuhle, J. et al. Conversion from clinically isolated syndrome to multiple sclerosis: a large multicentre study. *Multiple Sclerosis Journal.* **21** (8), 1013-1024 (2015).

13 El-Khatib, A. H. et al. Gadolinium in human brain sections and colocalization with other elements. *Neurology: Neuroimmunology & Neuroinflammation.* **6** (1), e515 (2019).
14 McDonald, R. J. et al. Intracranial Gadolinium Deposition after Contrast-enhanced MR Imaging. *Radiology.* **275** (3), 772-782 (2015).
15 McDonald, R. J. et al. Gadolinium Deposition in Human Brain Tissues after Contrast-enhanced MR Imaging in Adult Patients without Intracranial Abnormalities. *Radiology.* **285** (2), 546-554 (2017).
16 Schlemm, L. et al. Gadopentetate but not gadobutrol accumulates in the dentate nucleus of multiple sclerosis patients. *Multiple Sclerosis.* **23** (7), 963-972 (2017).
17 Boyken, J., Niendorf, T., Flemming, B., Seeliger, E. Gadolinium Deposition in the Brain after Contrast-enhanced MRI: Are the Data Valid? *Radiology.* **288** (2), 630-632 (2018).
18 Rovira, À. et al. MAGNIMS consensus guidelines on the use of MRI in multiple sclerosis—clinical implementation in the diagnostic process. *Nature Reviews Neurology.* **11**, 471 (2015).
19 Wattjes, M. P. et al. MAGNIMS consensus guidelines on the use of MRI in multiple sclerosis—establishing disease prognosis and monitoring patients. *Nature Reviews Neurology.* **11** (10), 597-606 (2015).
20 Traboulsee, A. et al. Revised Recommendations of the Consortium of MS Centers Task Force for a Standardized MRI Protocol and Clinical Guidelines for the Diagnosis and Follow-Up of Multiple Sclerosis. *American Journal of Neuroradiology .* **37** (3), 394-401 (2016).
21 Sąsiadek, M. et al. Recommendations of the Polish Medical Society of Radiology and the Polish Society of Neurology for the routinely used magnetic resonance imaging protocol in patients with multiple sclerosis. *Polish Journal of Radiology.* **85** e272-e276 (2020).
22 Maranzano, J. et al. Comparison of multiple sclerosis cortical lesion types detected by multicontrast 3T and 7T MRI. *American Journal of Neuroradiology.* **40** (7), 1162-1169 (2019).
23 Arevalo, O., Riascos, R., Rabiei, P., Kamali, A., Nelson, F. Standardizing Magnetic Resonance Imaging Protocols, Requisitions, and Reports in Multiple Sclerosis: An Update for Radiologist Based on 2017 Magnetic Resonance Imaging in Multiple Sclerosis and 2018 Consortium of Multiple Sclerosis Centers Consensus Guidelines. *Journal of Computer Assisted Tomography.* **43** (1), 1-12 (2019).
24 Schmierer, K. et al. Towards a standard MRI protocol for multiple sclerosis across the UK. *The British Journal of Radiology.* **92** (1101), 20180926 (2019).
25 Pereira, D. J. et al. Consensus Recommendations of the Multiple Sclerosis Study Group and the Portuguese Neuroradiological Society for the Use of Magnetic Resonance Imaging in Multiple Sclerosis in Clinical Practice: Part 2. *Acta Médica Portuguesa.* **33** (1), 66-75 (2020).
26 Zivadinov, R., Bakshi, R. Role of MRI in multiple sclerosis I: inflammation and lesions. *Front Biosci.* **9** (665), C28 (2004).
27 Hemond, C. C., Bakshi, R. Magnetic resonance imaging in multiple sclerosis. *Cold Spring Harbor Perspectives in Medicine.* **8** (5), a028969 (2018).
28 Thompson, A. J. et al. Diagnosis of multiple sclerosis: 2017 revisions of the McDonald criteria. *The Lancet Neurology.* **17** (2), 162-173 (2018).
29 Neema, M. et al. T1-and T2-based MRI measures of diffuse gray matter and white matter damage in patients with multiple sclerosis. *Journal of Neuroimaging.* **17**, 16S-21S (2007).
30 Shepherd, T. M. et al. New rapid, accurate T(2) quantification detects pathology in normal-appearing brain regions of relapsing-remitting MS patients. *NeuroImage. Clinical.* **14**, 363-370 (2017).

31 Tallantyre, E. C. et al. A comparison of 3T and 7T in the detection of small parenchymal veins within MS lesions. *Investigative Radiology.* **44** (9), 491-494 (2009).
32 Geraldes, R. et al. The current role of MRI in differentiating multiple sclerosis from its imaging mimics. *Nature Reviews Neurology.* **14** (4), 199 (2018).
33 Sinnecker, T. et al. Evaluation of the Central Vein Sign as a Diagnostic Imaging Biomarker in Multiple Sclerosis. *JAMA Neurology.* **76** (12), 1446-1456 (2019).
34 Bagnato, F. et al. Untangling the R2* contrast in multiple sclerosis: a combined MRI-histology study at 7.0 Tesla. *Public Library of Science one.* **13** (3), (2018).
35 Walsh, A. J. et al. Multiple sclerosis: validation of MR imaging for quantification and detection of iron. *Radiology.* **267** (2), 531-542 (2013).
36 Bozin, I. et al. Magnetic resonance phase alterations in multiple sclerosis patients with short and long disease duration. *Public Library of Science one.* **10** (7), e0128386 (2015).
37 Ropele, S. et al. Determinants of iron accumulation in deep grey matter of multiple sclerosis patients. *Multiple Sclerosis Journal.* **20** (13), 1692-1698 (2014).
38 Walsh, A. J. et al. Longitudinal MR imaging of iron in multiple sclerosis: an imaging marker of disease. *Radiology.* **270** (1), 186-196 (2014).
39 Blazejewska, A. I. et al. Increase in the iron content of the substantia nigra and red nucleus in multiple sclerosis and clinically isolated syndrome: a 7 Tesla MRI study. *Journal of Magnetic Resonance Imaging.* **41** (4), 1065-1070 (2015).
40 Bonnier, G. et al. Advanced MRI unravels the nature of tissue alterations in early multiple sclerosis. *Annals of Clinical and Translational Neurology.* **1** (6), 423-432 (2014).
41 Niendorf, T., Barth, M., Kober, F., Trattnig, S. From ultrahigh to extreme field magnetic resonance: where physics, biology and medicine meet. *MAGMA* **29** (3), 309-311 (2016).
42 Sinnecker, T. et al. Ultrahigh field MRI in clinical neuroimmunology: a potential contribution to improved diagnostics and personalised disease management. *EPMA.* **6** (1), 16, doi:10.1186/s13167-015-0038-y, (2015).
43 Vaughan, J. T. et al. 7T vs. 4T: RF power, homogeneity, and signal-to-noise comparison in head images. *Magnetic Resonance in Medicine.* **46** (1), 24-30 (2001).
44 Padormo, F., Beqiri, A., Hajnal, J. V., Malik, S. J. Parallel transmission for ultrahigh-field imaging. *NMR in Biomedicine.* **29** (9), 1145-1161 (2016).
45 Bruschi, N., Boffa, G., Inglese, M. Ultra-high-field 7-T MRI in multiple sclerosis and other demyelinating diseases: from pathology to clinical practice. *European Radiology Experimental.* **4** (1), 59 (2020).
46 Sati, P. et al. The central vein sign and its clinical evaluation for the diagnosis of multiple sclerosis: a consensus statement from the North American Imaging in Multiple Sclerosis Cooperative. *Nature Reviews Neurology.* **12** (12), 714-722 (2016).
47 Tan, I. L. et al. MR venography of multiple sclerosis. *American Journal of Neuroradiology* . **21** (6), 1039-1042 (2000).
48 Maggi, P. et al. The formation of inflammatory demyelinated lesions in cerebral white matter. *Annals of Neurology.* **76** (4), 594-608 (2014).
49 Tallantyre, E. C. et al. A comparison of 3T and 7T in the detection of small parenchymal veins within MS lesions. *Investigative Radiology.* **44** (9), 491-494 (2009).
50 Filippi, M. et al. Assessment of lesions on magnetic resonance imaging in multiple sclerosis: practical guidelines. *Brain.* **142** (7), 1858-1875 (2019).
51 Muller, K. et al. Detailing intra-lesional venous lumen shrinking in multiple sclerosis investigated by sFLAIR MRI at 7-T. *Journal of Neurology* (2014).

52 Sinnecker, T. et al. Periventricular venous density in multiple sclerosis is inversely associated with T2 lesion count: a 7 Tesla MRI study. *Multiple Sclerosis.* **19** (3), 316-325 (2013).
53 Wuerfel, J. et al. Lesion morphology at 7 Tesla MRI differentiates Susac syndrome from multiple sclerosis. *Multiple Sclerosis.* **18** (11), 1592-1599 (2012).
54 Sinnecker, T. et al. Distinct lesion morphology at 7-T MRI differentiates neuromyelitis optica from multiple sclerosis. *Neurology.* **79** (7), 708-714 (2012).
55 Kuchling, J. et al. Identical lesion morphology in primary progressive and relapsing-remitting MS--an ultrahigh field MRI study. *Multiple Sclerosis.* **20** (14), 1866-1871 (2014).
56 Sinnecker, T. et al. Multiple sclerosis lesions and irreversible brain tissue damage: a comparative ultrahigh-field strength magnetic resonance imaging study. *Archives of Neurology.* **69** (6), 739-745 (2012).
57 Behrens, J. R. et al. 7 Tesla MRI of Balo's concentric sclerosis versus multiple sclerosis lesions. *Annals of Clinical and Translational Neurology.* **5** (8), 900-912 (2018).
58 Blaabjerg, M. et al. Widespread inflammation in CLIPPERS syndrome indicated by autopsy and ultra-high-field 7T MRI. *Neurology: Neuroimmunology & Neuroinflammation.* **3** (3), e226 (2016).
59 Noureddine, Y. et al. Experience with magnetic resonance imaging of human subjects with passive implants and tattoos at 7 T: a retrospective study. *Magnetic Resonance Materials in Physics, Biology and Medicine.* **28** (6), 577-590 (2015).
60 Kraff, O., Quick, H. H. 7T: Physics, safety, and potential clinical applications. *Journal of Magnetic Resonance Imaging.* **46** (6), 1573-1589 (2017).
61 Hoff, M. N. et al. Safety Considerations of 7-T MRI in Clinical Practice. *Radiology.* **292** (3), 509-518 (2019).
62 Kraff, O., Quick, H. H. Sicherheit von Implantaten im Hochfeld- und Ultrahochfeld-MRT. *Der Radiologe.* **59** (10), 898-905 (2019).
63 Fagan, A. J. et al. 7T MR Safety. *Journal of Magnetic Resonance Imaging.* (2020).
64 Technologists, T. I. S. f. M. R. i. M. a. T. S. f. M. R. *MR Safety Guidance, Documents and Links: MR Safety Strategies to Help You Stay Current with MR Safety Standards*, <https://www.ismrm.org/mr-safety-links/mr-safety-resources-page/> (2020).
65 Versluis, M. J. et al. Subject tolerance of 7 T MRI examinations. *Journal of Magnetic Resonance Imaging.* **38** (3), 722-725 (2013).
66 Theysohn, J. M. et al. Subjective acceptance of 7 Tesla MRI for human imaging. *Magnetic Resonance Materials in Physics, Biology and Medicine.* **21** (1-2), 63 (2008).
67 Klix, S. et al. On the Subjective Acceptance during Cardiovascular Magnetic Resonance Imaging at 7.0 Tesla. *PLoS One.* **10** (1), e0117095 (2015).
68 Rauschenberg, J. et al. Multicenter study of subjective acceptance during magnetic resonance imaging at 7 and 9.4 T. *Investigative Radiology.* **49** (5), 249-259 (2014).
69 Zurawski, J., Lassmann, H., Bakshi, R. Use of Magnetic Resonance Imaging to Visualize Leptomeningeal Inflammation in Patients With Multiple Sclerosis: A Review. *JAMA Neurologyogy.* **74** (1), 100-109 (2017).
70 Radue, E.-W. et al. Correlation between brain volume loss and clinical and MRI outcomes in multiple sclerosis. *Neurology.* **84** (8), 784-793 (2015).
71 Filippi, M. et al. A high-resolution three-dimensional T1-weighted gradient echo sequence improves the detection of disease activity in multiple sclerosis. *Annals of Neurology.* **40** (6), 901-907 (1996).

72 Mugler III, J. P., Brookeman, J. R. Three-dimensional magnetization-prepared rapid gradient-echo imaging (3D MP RAGE). *Magnetic Resonance in Medicine.* **15** (1), 152-157 (1990).
73 Lindig, T. et al. Evaluation of multimodal segmentation based on 3D T1-, T2- and FLAIR-weighted images – the difficulty of choosing. *NeuroImage.* **170**, 210-221 (2018).
74 Nelson, F., Poonawalla, A., Hou, P., Wolinsky, J. S., Narayana, P. A. 3D MPRAGE improves classification of cortical lesions in multiple sclerosis. *Multiple sclerosis (Houndmills, Basingstoke, England).* **14** (9), 1214-1219 (2008).
75 Marques, J. P. et al. MP2RAGE, a self bias-field corrected sequence for improved segmentation and T1-mapping at high field. *NeuroImage.* **49** (2), 1271-1281 (2010).
76 Kober, T. et al. MP2RAGE Multiple Sclerosis Magnetic Resonance Imaging at 3 T. *Investigative Radiology.* **47** (6), 346-352 (2012).
77 Beck, E. S. et al. Improved Visualization of Cortical Lesions in Multiple Sclerosis Using 7T MP2RAGE. *American Journal of Neuroradiology.* **39** (3), 459-466 (2018).
78 Bø, L., Vedeler, C. A., Nyland, H. I., Trapp, B. D., Mørk, S. J. Subpial Demyelination in the Cerebral Cortex of Multiple Sclerosis Patients. *Journal of Neuropathology*, *Experimental Neurology.* **62** (7), 723-732 (2003).
79 Kilsdonk, I. D. et al. Increased cortical grey matter lesion detection in multiple sclerosis with 7 T MRI: a post-mortem verification study. *Brain.* **139** (5), 1472-1481 (2016).
80 Absinta, M. et al. Gadolinium-based MRI characterization of leptomeningeal inflammation in multiple sclerosis. *Neurology.* **85** (1), 18-28 (2015).
81 Titelbaum, D. S. et al. Leptomeningeal Enhancement on 3D-FLAIR MRI in Multiple Sclerosis: Systematic Observations in Clinical Practice. *Journal of Neuroimaging.* **30** (6), 917-929 (2020).
82 Schmidt, P. et al. Automated segmentation of changes in FLAIR-hyperintense white matter lesions in multiple sclerosis on serial magnetic resonance imaging. *NeuroImage: Clinical.* **23**, 101849 (2019).
83 Coulette, S. et al. Diagnosis and Prediction of Relapses in Susac Syndrome: A New Use for MR Postcontrast FLAIR Leptomeningeal Enhancement. *American Journal of Neuroradiology.* **40** (7), 1184-1190 (2019).
84 Cohen-Adad, J. et al. T2* mapping and B0 orientation-dependence at 7T reveal cyto- and myeloarchitecture organization of the human cortex. *NeuroImage.* **60** (2), 1006-1014 (2012).
85 Louapre, C. et al. The association between intra- and juxta-cortical pathology and cognitive impairment in multiple sclerosis by quantitative T2* mapping at 7T MRI. *NeuroImage: Clinical.* **12**, 879-886 (2016).
86 Liu, S. et al. Susceptibility-weighted imaging: current status and future directions. *NMR in Biomedicine.* **30** (4), e3552 (2017).
87 Haacke, E. M., Xu, Y., Cheng, Y. C., Reichenbach, J. R. Susceptibility weighted imaging (SWI). *Magnetic Resonance in Medicine.* **52** (3), 612-618 (2004).
88 Haacke, E. M. et al. Characterizing iron deposition in multiple sclerosis lesions using susceptibility weighted imaging. *Journal of Magnetic Resonance Imaging.* **29** (3), 537-544 (2009).
89 Pitt, D. et al. Imaging Cortical Lesions in Multiple Sclerosis With Ultra–High-Field Magnetic Resonance Imaging. *Archives of Neurology.* **67** (7), 812-818 (2010).
90 Li, X. et al. Magnetic susceptibility contrast variations in multiple sclerosis lesions. *Journal of Magnetic Resonance Imaging.* **43** (2), 463-473 (2016).

91 Dal-Bianco, A. et al. Slow expansion of multiple sclerosis iron rim lesions: pathology and 7 T magnetic resonance imaging. *Acta Neuropathologica.* **133** (1), 25-42 (2017).
92 Sati, P. Diagnosis of multiple sclerosis through the lens of ultra-high-field MRI. *Journal of Magnetic Resonance.* **291**, 101-109 (2018).
93 Griswold, M. A. et al. Generalized autocalibrating partially parallel acquisitions (GRAPPA). *Magnetic Resonance in Medicine.* **47** (6), 1202-1210 (2002).
94 Hammond, K. E. et al. Development of a robust method for generating 7.0 T multichannel phase images of the brain with application to normal volunteers and patients with neurological diseases. *NeuroImage.* **39** (4), 1682-1692 (2008).
95 Haacke, E. M. et al. Quantitative susceptibility mapping: current status and future directions. *Magnetic Resonance Imaging.* **33** (1), 1-25 (2015).
96 Langkammer, C. et al. Quantitative susceptibility mapping in multiple sclerosis. *Radiology.* **267** (2), 551-559 (2013).
97 Eskreis-Winkler, S. et al. Multiple sclerosis lesion geometry in quantitative susceptibility mapping (QSM) and phase imaging. *Journal of Magnetic Resonance Imaging.* **42** (1), 224-229 (2015).
98 Chawla, S. et al. Longitudinal study of multiple sclerosis lesions using ultra-high field (7T) multiparametric MR imaging. *PLOS ONE.* **13** (9), e0202918 (2018).
99 Kolasinski, J. et al. A combined post-mortem magnetic resonance imaging and quantitative histological study of multiple sclerosis pathology. *Brain.* **135** (10), 2938-2951 (2012).
100 De Santis, S. et al. Evidence of early microstructural white matter abnormalities in multiple sclerosis from multi-shell diffusion MRI. *NeuroImage: Clinical.* **22**, 101699 (2019).
101 Filippi, M. et al. Microstructural magnetic resonance imaging of cortical lesions in multiple sclerosis. *Multiple Sclerosis.* **19** (4), 418-426 (2013).
102 Granberg, T. et al. In vivo characterization of cortical and white matter neuroaxonal pathology in early multiple sclerosis. *Brain: a Journal of Neurology.* **140** (11), 2912-2926 (2017).
103 Holland, D., Kuperman, J. M., Dale, A. M. Efficient correction of inhomogeneous static magnetic field-induced distortion in Echo Planar Imaging. *NeuroImage.* **50** (1), 175-183 (2010).
104 In, M.-H., Posnansky, O., Beall, E. B., Lowe, M. J., Speck, O. Distortion correction in EPI using an extended PSF method with a reversed phase gradient approach. *PloS one.* **10** (2), e0116320-e0116320 (2015).
105 Van de Moortele, P. F. et al. B(1) destructive interferences and spatial phase patterns at 7 T with a head transceiver array coil. *Magnetic Resonance in Medicine.* **54** (6), 1503-1518 (2005).
106 Collins, C. M., Liu, W., Schreiber, W., Yang, Q. X., Smith, M. B. Central brightening due to constructive interference with, without, and despite dielectric resonance. *Journal of Magnetic Resonance Imaging.* **21** (2), 192-196 (2005).
107 Yang, Q. X. et al. Manipulation of image intensity distribution at 7.0 T: passive RF shimming and focusing with dielectric materials. *Journal of Magnetic Resonance Imaging.* **24** (1), 197-202 (2006).
108 Teeuwisse, W. M., Brink, W. M., Webb, A. G. Quantitative assessment of the effects of high-permittivity pads in 7 Tesla MRI of the brain. *Magnetic Resonance in Medicine.* **67** (5), 1285-1293 (2012).

109 van Gemert, J., Brink, W., Webb, A., Remis, R. High-permittivity pad design tool for 7T neuroimaging and 3T body imaging. *Magnetic Resonance in Medicine.* **81** (5), 3370-3378 (2019).
110 Vaidya, M. V. et al. Improved detection of fMRI activation in the cerebellum at 7T with dielectric pads extending the imaging region of a commercial head coil. *Journal of Magnetic Resonance Imaging.* **48** (2), 431-440 (2018).
111 Brink, W. M., van der Jagt, A. M., Versluis, M. J., Verbist, B. M., Webb, A. G. High permittivity dielectric pads improve high spatial resolution magnetic resonance imaging of the inner ear at 7 T. *Investigative Radiology.* **49** (5), 271-277 (2014).
112 Lundkvist, M. et al. Characterization of anti-natalizumab antibodies in multiple sclerosis patients. *Multiple Sclerosis.* **19** (6), 757-764 (2013).
113 Moccia, M. et al. Advances in spinal cord imaging in multiple sclerosis. *Therapeutic Advances in Neurological Disorders.* **12**, 1756286419840593-1756286419840593, doi:10.1177/1756286419840593, (2019).
114 Zhao, W. et al. Nineteen-channel receive array and four-channel transmit array coil for cervical spinal cord imaging at 7T. *Magnetic Resonance in Medicine.* **72** (1), 291-300 (2014).
115 Sinnecker, T. et al. MRI phase changes in multiple sclerosis vs neuromyelitis optica lesions at 7T. *Neurology: Neuroimmunology & Neuroinflammation.* **3** (4), e259 (2016).
116 Wenz, D. et al. Millimeter spatial resolution in vivo sodium MRI of the human eye at 7 T using a dedicated radiofrequency transceiver array. *Magnetic Resonance in Medicine.* **80** (2), 672-684 (2018).
117 Huhn, K., Engelhorn, T., Linker, R. A., Nagel, A. M. Potential of Sodium MRI as a Biomarker for Neurodegeneration and Neuroinflammation in Multiple Sclerosis. *Frontiers in Neurology.* **10** (84) (2019).
118 Bolo, N. R. et al. Brain Pharmacokinetics and Tissue Distribution In Vivo of Fluvoxamine and Fluoxetine by Fluorine Magnetic Resonance Spectroscopy. *Neuropsychopharmacology.* **23** (4), 428-438 (2000).
119 Ji, Y. et al. Eight-channel transceiver RF coil array tailored for 1H/19F MR of the human knee and fluorinated drugs at 7.0 T. *NMR in Biomedicine.* **28** (6), 726-737 (2015).
120 Starke, L., Pohlmann, A., Prinz, C., Niendorf, T., Waiczies, S. Performance of compressed sensing for fluorine-19 magnetic resonance imaging at low signal-to-noise ratio conditions. *Magnetic Resonance in Medicine.* 1-17 (2019).

Figure 1

Click here to access/download;Figure;Figure 1.eps

Figure 2

a b

Figure 3

Click here to access/download;Figure;Figure 3.eps

a

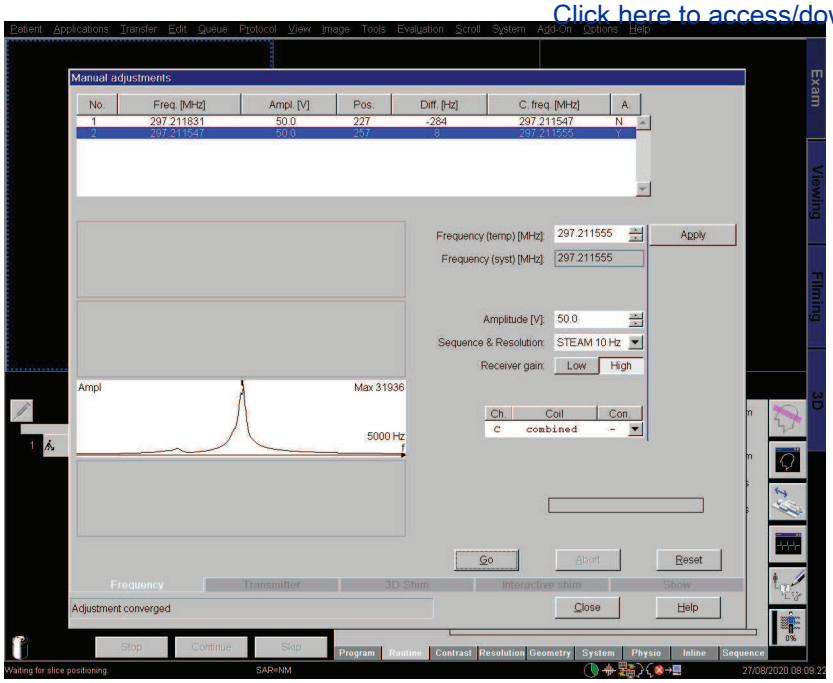

b

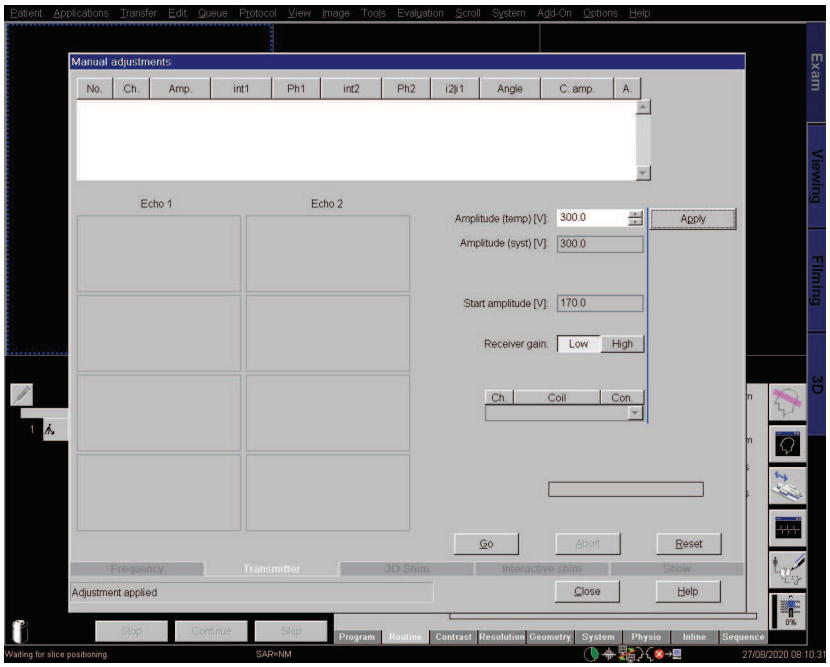

c

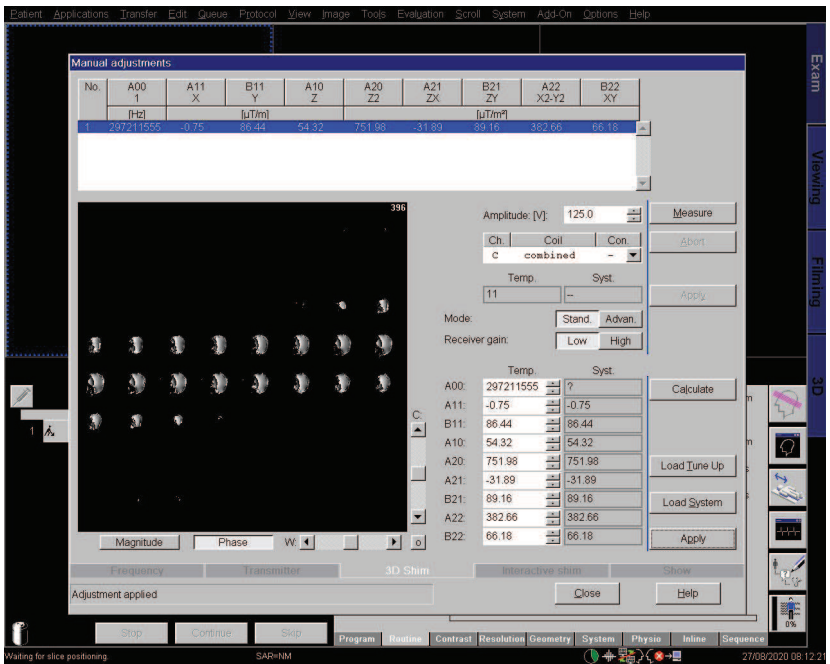

Figure 4

Click here to access/download;Figure;Figure 4.eps

a

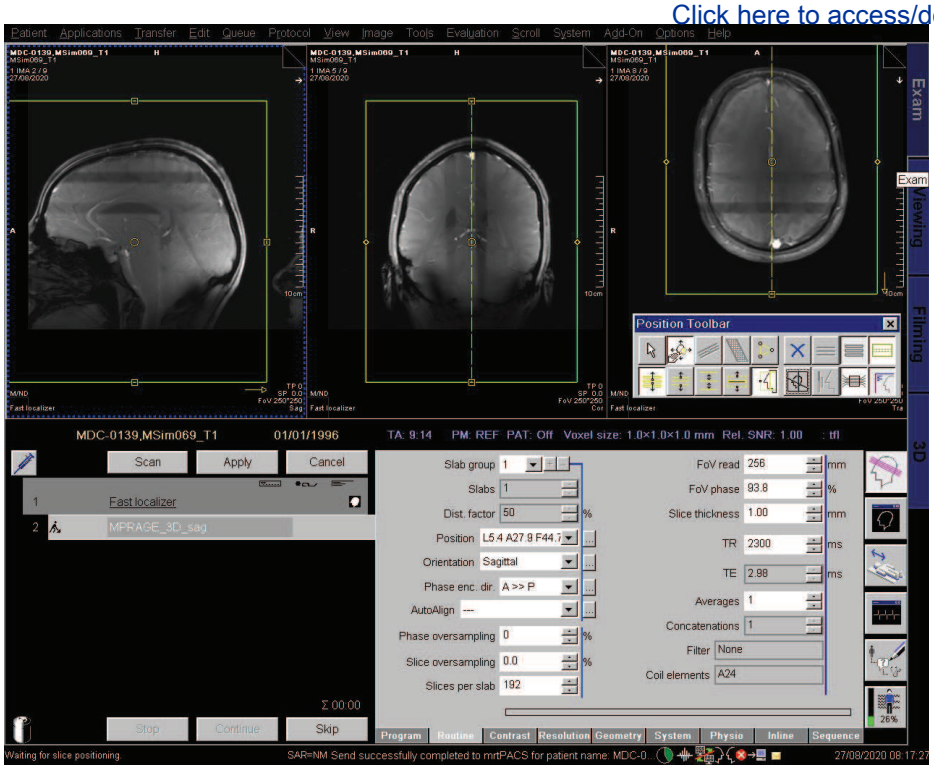

b

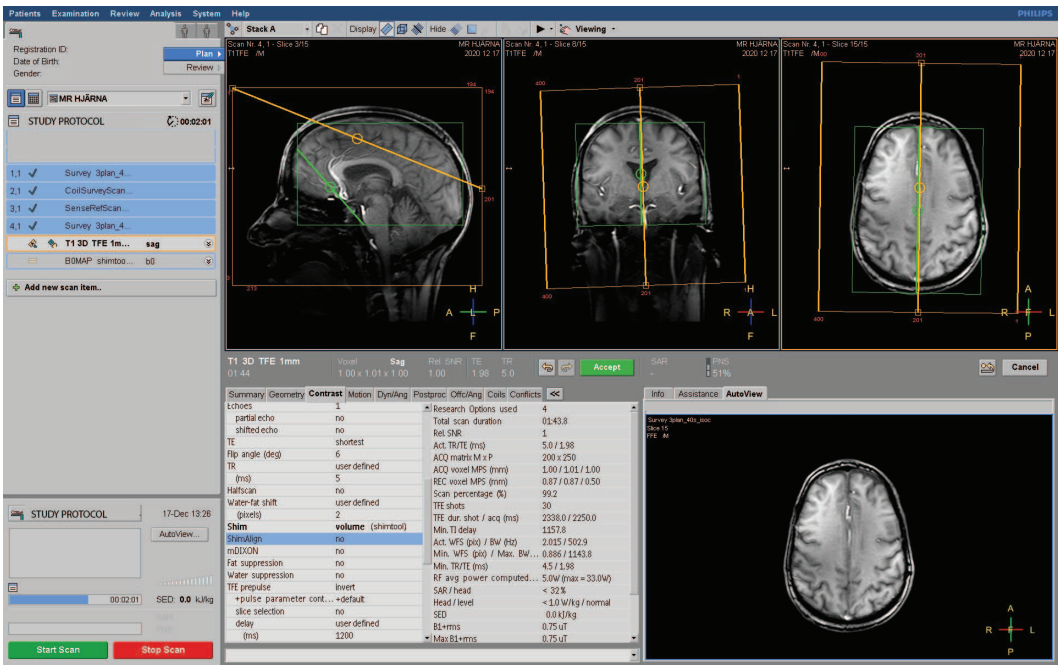

c

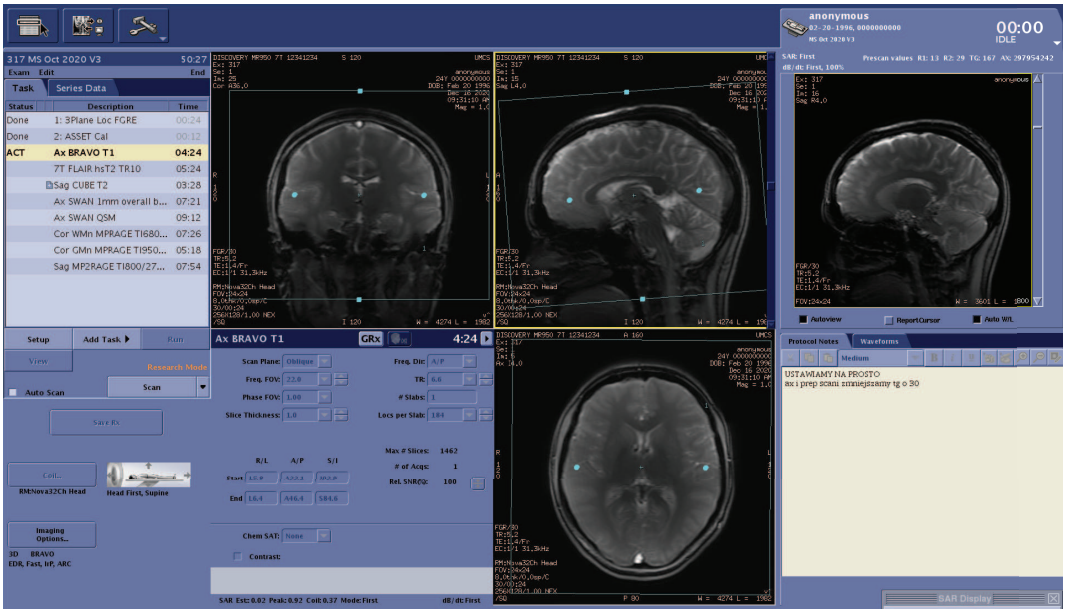

Figure 5

Click here to access/download;Figure;Figure 5.eps

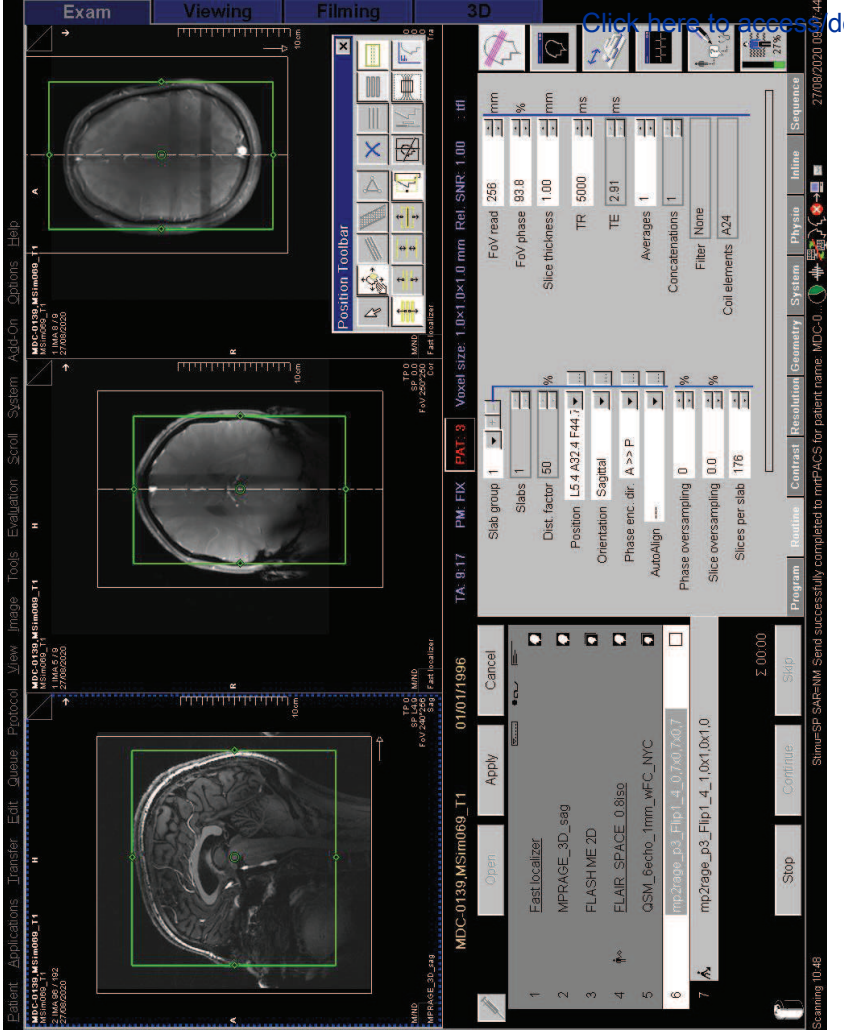

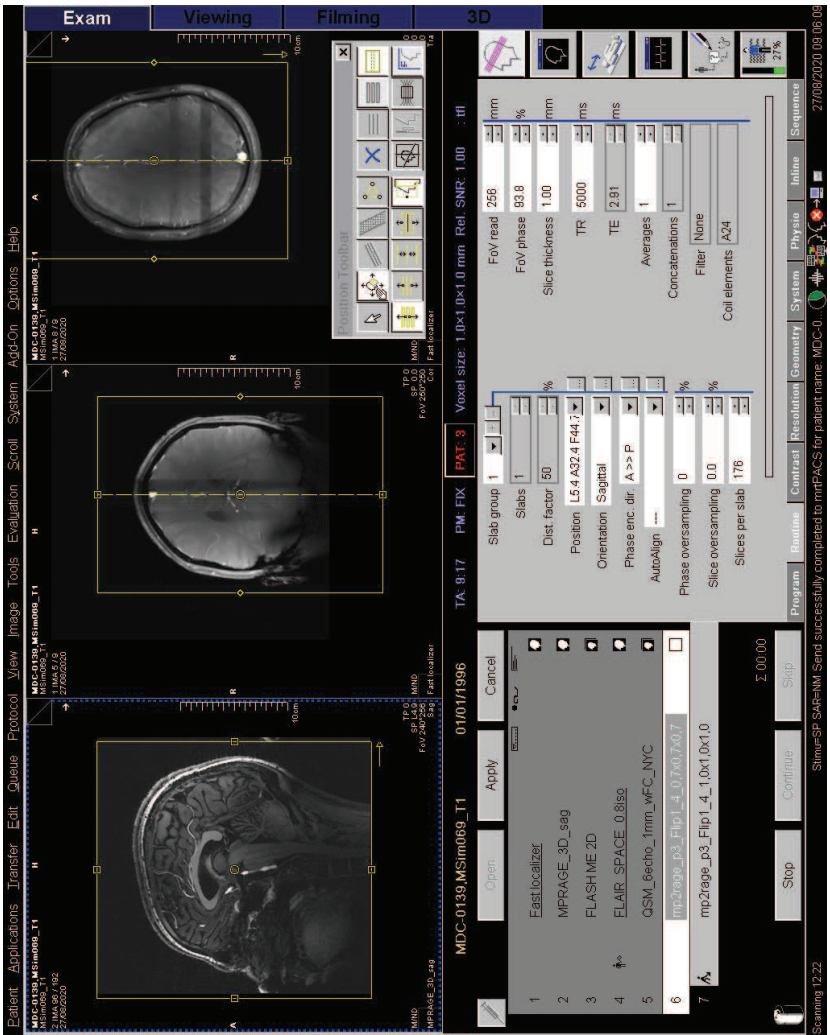

Figure 6

Click here to access/download;Figure;Figure 6.eps

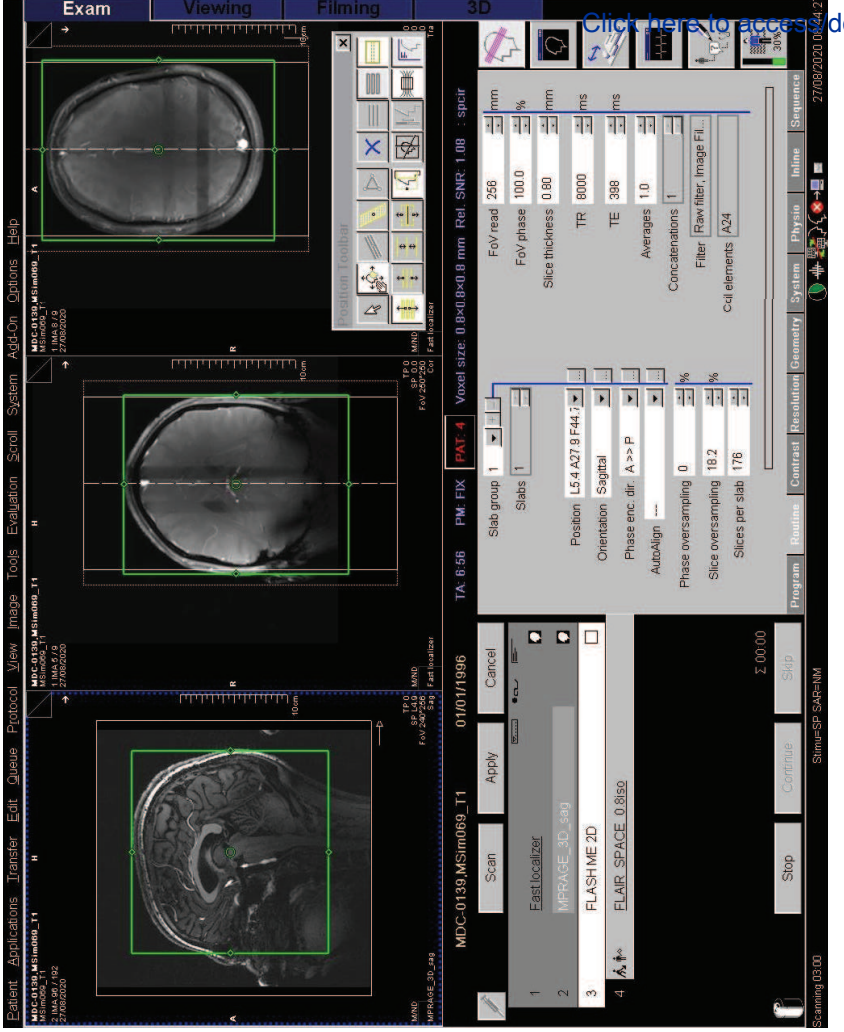

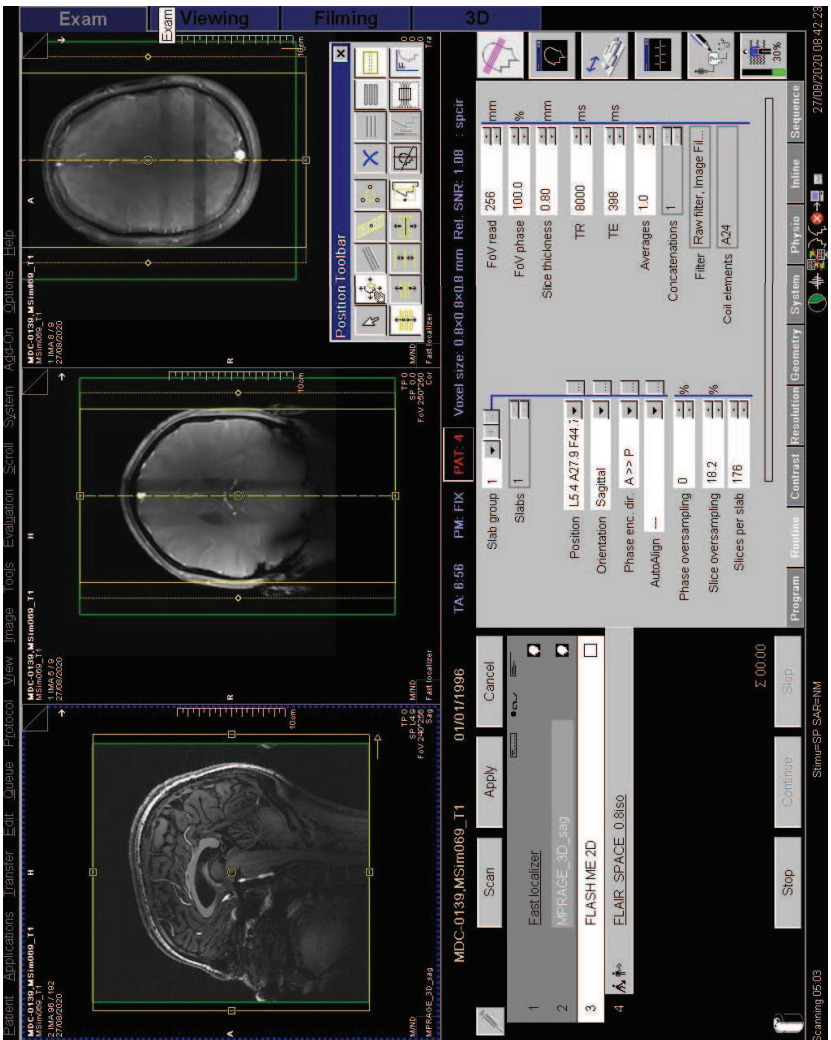

Figure 7

Click here to access/download;Figure;Figure 7.eps

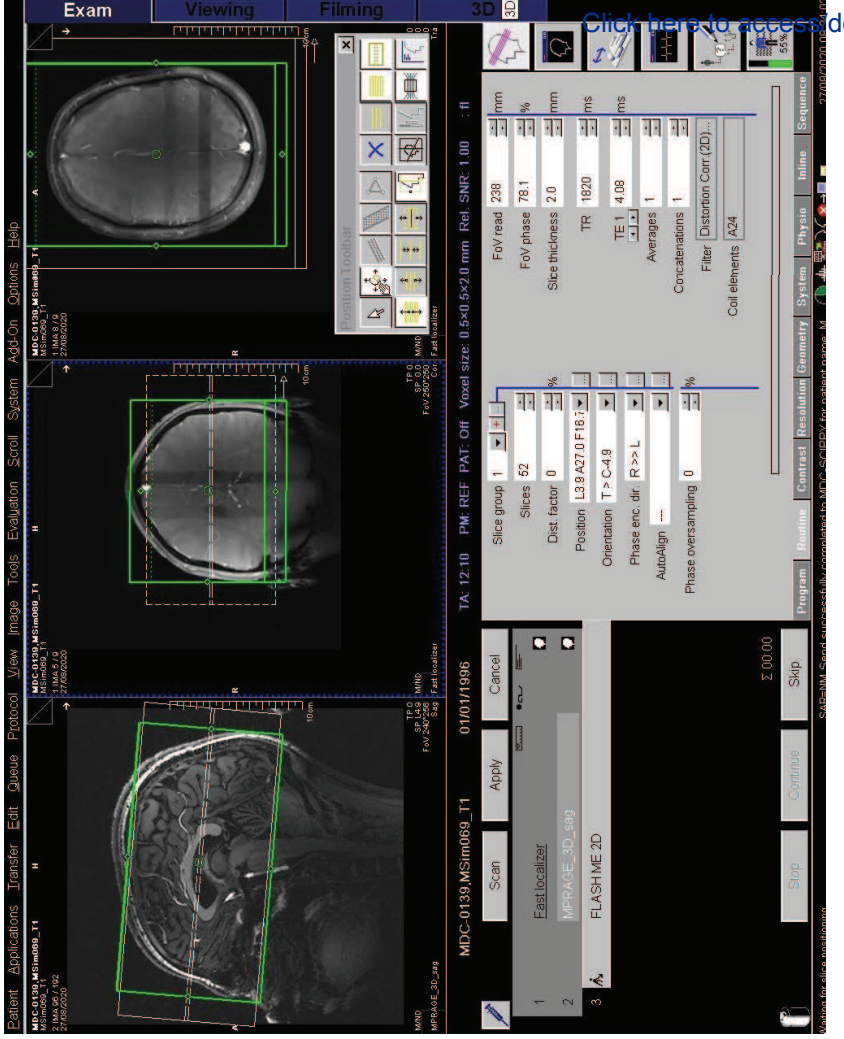

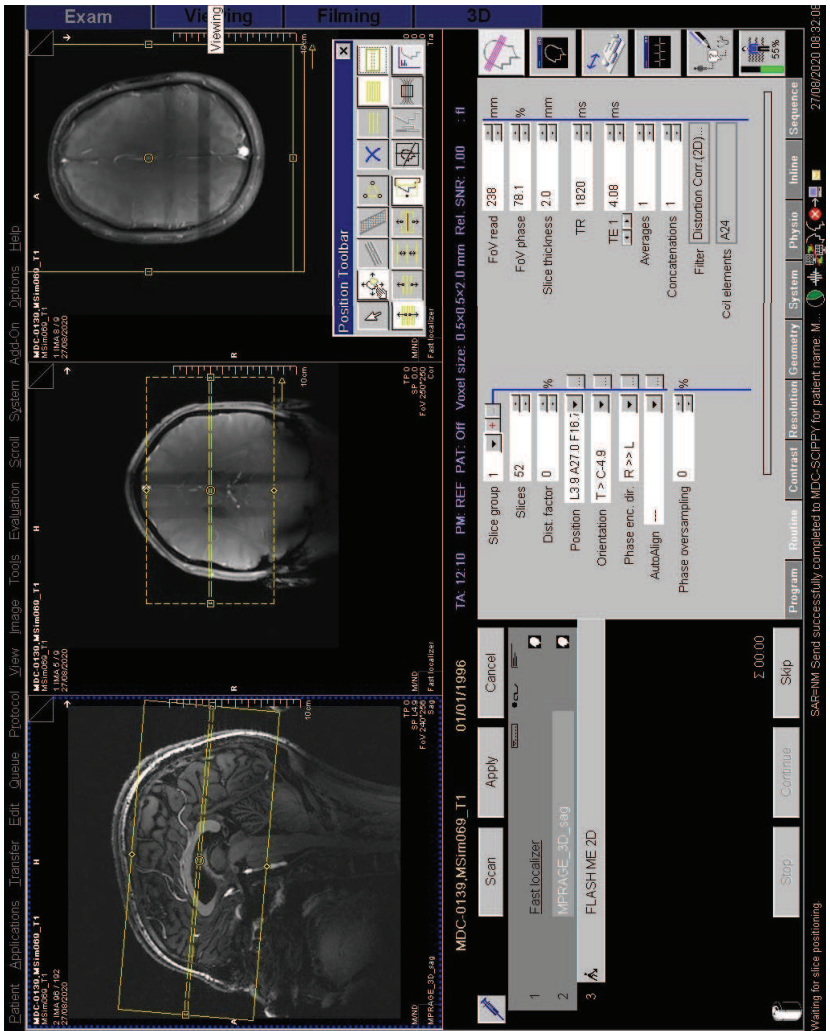

Figure 8

Click here to access/download;Figure;Figure 8.eps

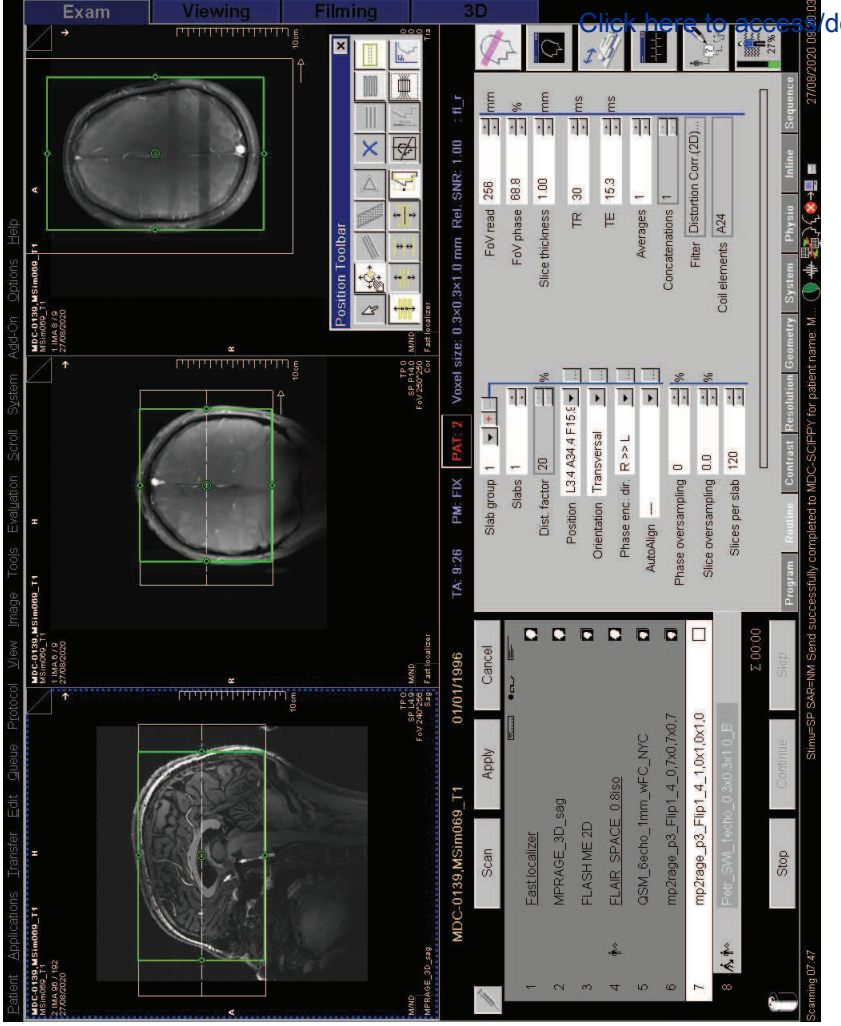

Figure 9

Click here to access/download;Figure;Figure 9.eps

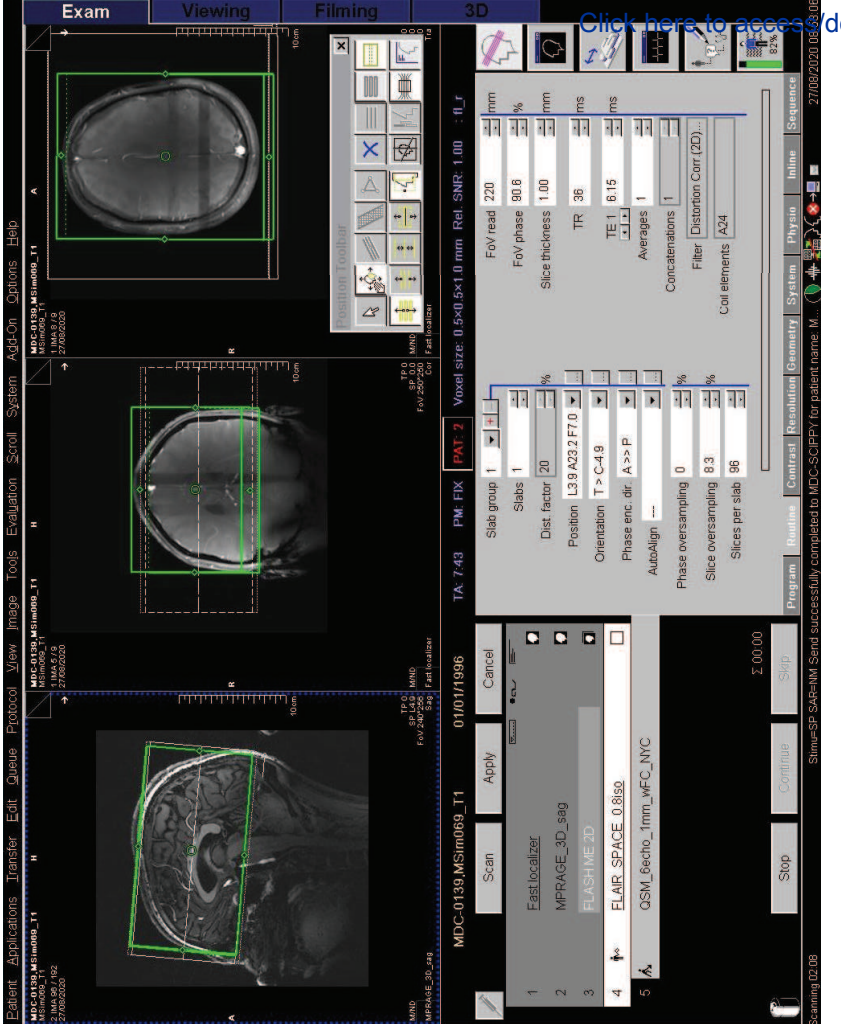

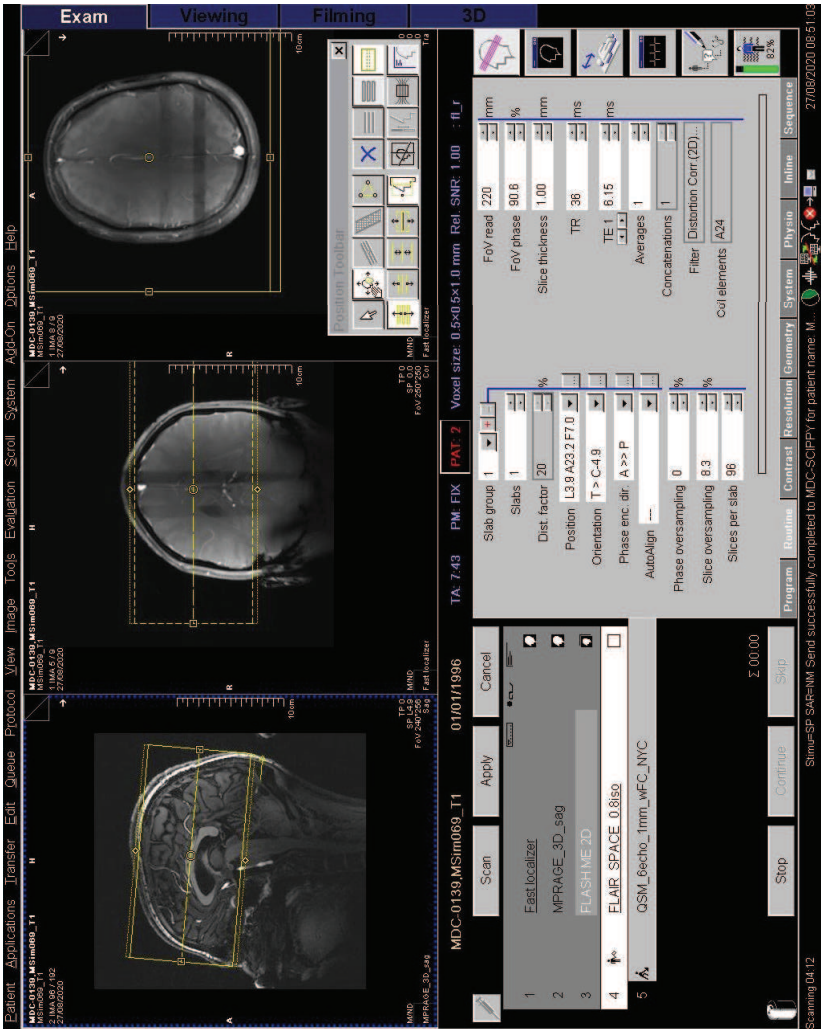

Figure 10

Click here to access/download;Figure;Figure 10.eps

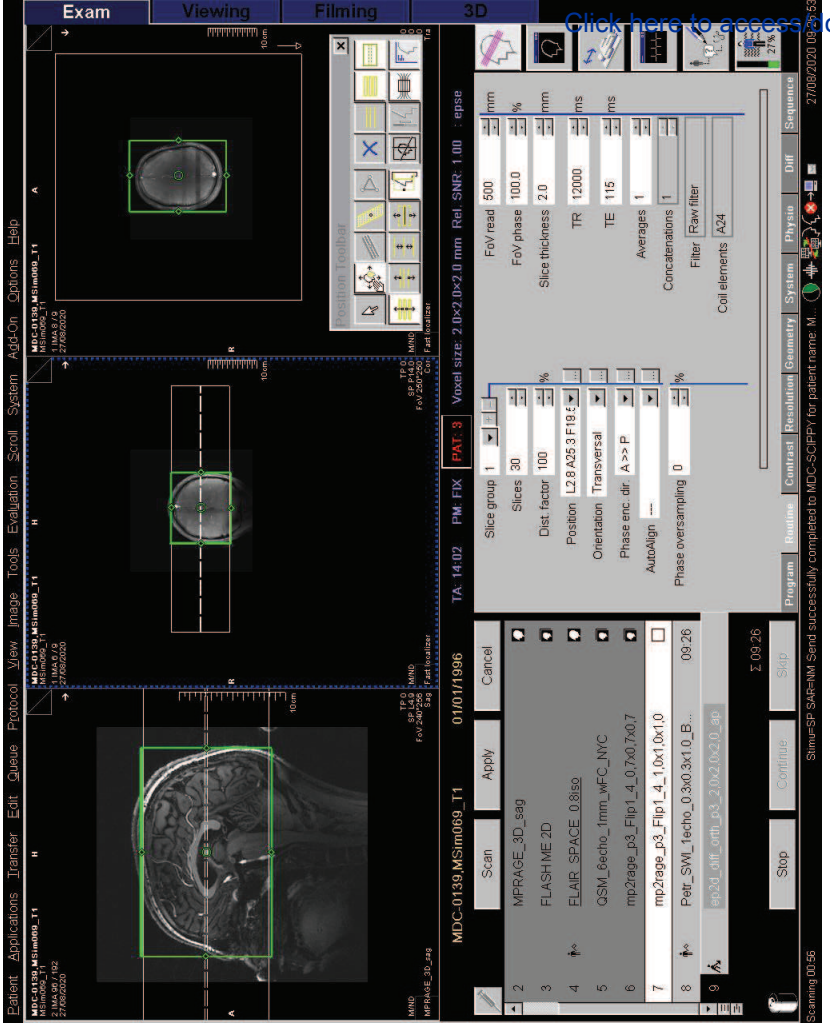

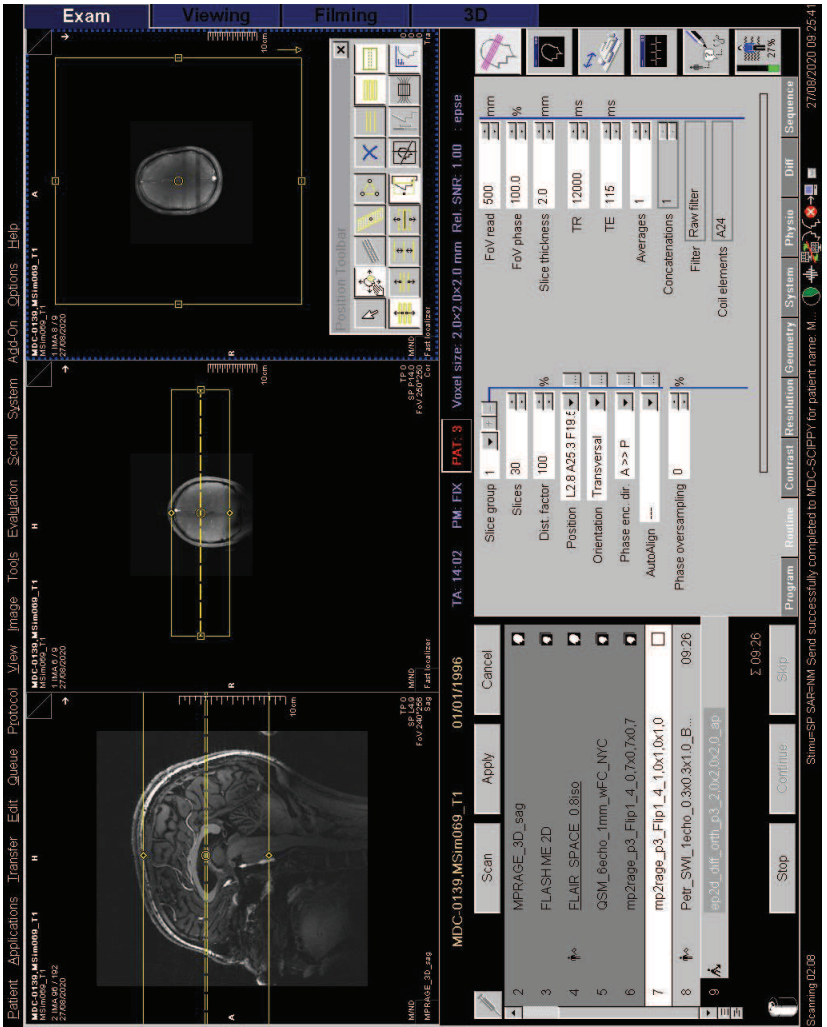

Figure 11

Figure 12

Figure 13

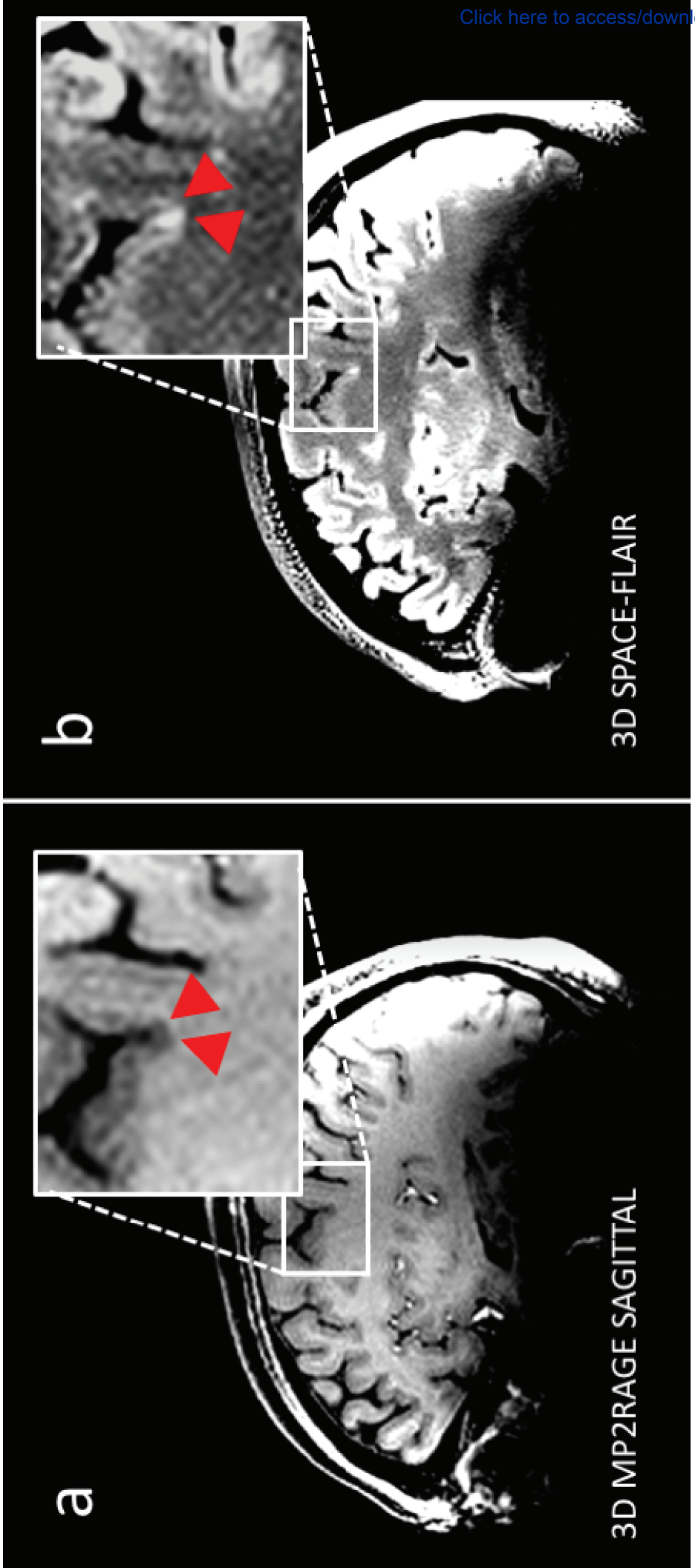

Figure 14

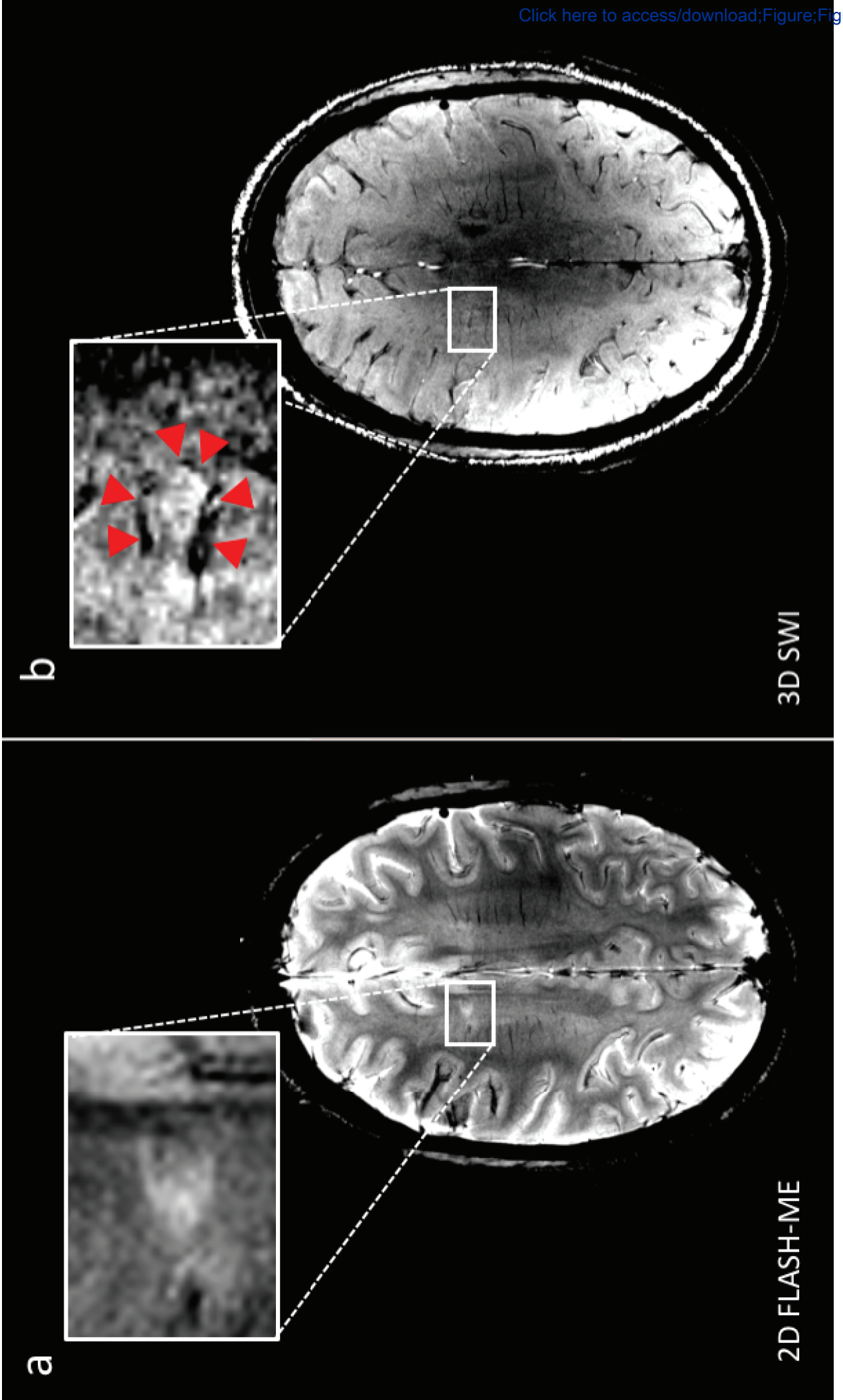

Metallic implants (can malfunction due to magnetic fields or cause injury)
Electronic devices e.g. pacemakers, defibrillators, insulin pump, nerve stimulators
Aneurysm and haemostatic clips, prosthetic heart valves
Cochlear, otologic implants
Drug infusion devices
Deep brain stimulation electrodes
Lead electrocardiogram wires
Other contraindications (risk of skin burns, swelling or damage via magnetic field effects)
Some medication patches
Metallic foreign bodies e.g. shrapnel or other minute metal fragments in the eye
Some tattoo and cosmetics (permanent makeup)
Body piercing jewellery
Pregnancy (possible adverse biological effects by magnetic fields)
Known claustrophobia

Table of Materials

Click here to access/download;Table of Materials;JoVE62142_Table_of_Materials.xlsx

Name of Material/Equipment	Company	Serial Number	Comments/Description
7T TX/RX 24 Ch Head Coil	Nova Medical, Inc., Wilmington, USA	NM008-24-7S-013	1-channel circular polarized (CP) transmit (Tx), 24-channel receive (Rx) RF head coil
Magnetom 7T System	Siemens Healthineers, Erlangen, Germany	MRB1076	7.0 T whole body research scanner
syngo MR B17 Software	Siemens Healthineers, Erlangen, Germany	B17A	image processing software for the Magnetom 7T system

MDC • Robert-Rössle-Straße 10 • 13125 Berlin

Dr. Sonia Waiczies

MDC Berlin-Buch
Max-Delbrück-Centrum für
Molekulare Medizin (MDC)
Robert-Rössle-Straße 10
13125 Berlin

Tel.: +49 (0)30 9406-4542
Fax: +49 (0)30 9406-49178

sonia.waiczies@mdc-berlin.de
www.mdc-berlin.de

Nam Nguyen, Ph.D.
Manager of Review
JoVE

22nd December 2020

JoVE62142:
Magnetic Resonance Imaging of Multiple Sclerosis at 7.0 Tesla

Dear Dr. Nguyen:

Thank you for reviewing the above manuscript and providing your feedback. We have made the changes that you and the reviewers have requested.

Please find uploaded a point-by-point response to the peer review comments and a revised version of the above manuscript.

Changes in the manuscript can be identified as colored text. Blue and green text reflects changes made in response to review 1 and review 2, respectively, and purple text reflects other changes following the editorial comments.

Approximately 3 pages of protocol text is highlighted in yellow for inclusion in the protocol section of the video.

We look forward to the next steps.

Yours sincerely,

Sonia Waiczies, Antje Els, Joseph Kuchling, Karin Markenroth Bloch, Anna Pankowska, Helmar Waiczies, Carl Herrmann, Claudia Chien, Carsten Finke, Friedemann Paul, Thoralf Niendorf

Reviewer #1

Major Concerns:

1. The manuscript is very detailed, to the point of excluding non-Siemens users. I feel that not all the details on adjustments and user interface are relevant, and they risk confusing other users (for example, but not limited to, 4.5-4.16). The large amount of detail also hides the important and more specific information regarding the UHF scanning and/or MS protocol. It would improve the accessibility of the paper if some of details were pruned away. I think you can refer the reader to the scanners user manual, for example. I think the manuscript would gain from focusing on the details that are UHF and/or MS specific and not the ones that are valid for all MR scanning.

   In order to avoid excluding non-Siemens MR users, we removed detail that was too specific to this MR system. We specify where the operation of a 7.0 T MR scanner might be different between different vendors. We also refer the reader to the operator manuals of their specific system. In addition, we include more detail specific to the MS pathology, particularly in the introduction of each MR acquisition method.

2. The manuscript discusses how to ask for and document contraindications and implants (Table 1, sections 1.1-2, 1.7) but gives no clear information on how to handle the information if a patient has an implant/device/tattoo. For example, Table 1 lists "Some tattoos" as contraindications, without any reference to in which circumstances tattoos are deemed safe or not. Overly conservative risk assessments are serious hindrance for patients to get potentially treatment changing UHF examinations, and it is important to in addition to discussing the serious risks of implants talk about what implants can be scanned without increased risk. At the least, a few references to recent published safety papers and guidelines should be included.

   We agree that overly conservative approaches might ultimately hinder the benefits that patient would otherwise gain from the examination. We have now added a note in the introduction of section 1. Subjects.

3. Regarding dedicated MR sequences; The rest of the manuscript is very detailed to the point of not changing angles of images stacks, but the sequences are as far as I understand just a list of sequences that can be used. The study protocol should define which sequences that are used (in 4.12 it says not to change anything as it will make data in longitudinal studies difficult to use - it would be even worse not to use the same scans?). How is it decided which sequences should be run?

   The sequences are run depending on the scientific or clinical question of the study e.g. the subtype or form of multiple sclerosis being studied. The sequences that we list in our protocol are the most commonly used in our MS clinical studies at 7.0 T. We have now sorted the sequences according to their contrast and have also included an informative section in the introduction of each sequence, indicating the significance and relevance of each specific sequence to the MS pathology.

4. Several of the MR sequences seem to give similar contrasts; 3D MPRAGE, 3D MP2RAGE and the four T2*-weighted sequences. It would add to the understanding if more information was added on why one sequence would be choosen over the other or how they give complementing information. it would also be interesting to see a list of the standard study protocol, which I assume will not contain all of the listed sequences.

We have now added more detail about each MR acquisition method in the opening section of each sequence, indicating the benefits of using one sequence over the others.

Minor Concerns:

5. P3 L69-70: Suggest to change to: "... resembling morphology at lower field strengths." to avoid the vague definition of "clinical field strength" as "typically =<3T.

   We changed the wording as suggested.

6. P4 L 82: Add a reference to parametric T2 mapping.

   We have added the reference from Shepherd and colleagues on T_2 qunatification to detect pathology in normal-appearing brain matter in relapsing-remitting MS patients.

7. P7 L164: I assume that I misunderstand this but; what is the point of locking valuables in a locker if the key is left in the locker? (Is this information even needed, it also seems like a detail which is not UHF specific)

   We removed this sentence.

8. P10 L235: "Walk slowly to the 7.0T examination table." - this requires an explanation of why you have to walk slowly.

   This protocol was written for a passively shielded magnet. We have added a sentence about passive versus active shielding (point 3.5).

9. P10 L237: "woolen blanket" - why does it have to be woolen?

   We have replaced “woolen blanket” with “blanket”

10. P13 4.12: This comment seems out of place - it concerns study design in general and is not specific to UHF (or MR in general) or MS.

    We removed this point.

11. P14 3D MPRAGE: Is the 1x1x1 mm3 acquisition really over 9 minutes? Why is no acceleration used?

    We have altered the protocol accordingly.

12. P14 4.20, 44: Why cant the angle be changed?

    While a strict sagittal setting is not absolutely necessary, it is recommended during longitudinal studies. One could alter the angle during planning and use anatomical structures as guides; these would then need to be implemented in the next examinations. Since it is a 3D sequence, the images can however still be registered onto the baseline scan. We have reworded this and introduced a sentence at the end of the MPRAGE sequence.

Reviewer #2

Major Concerns:

1. There is very little content both in the manuscript and protocol addressing B0 and B1 inhomogeneity and its impact on the scan quality and diagnostic accuracy. Attempts to mitigate these problems are not included in sufficient detail.

   We agree with the reviewer and now address B_1 inhomogeneities in "Representative Results" (see next points) and B_0 inhomogeneities in the section "Adjustments and scout images":

   4.4: "…. These include a correction (shimming) of the inhomogeneous static magnetic (B_0) field. B_0 inhomogeneities occur because of the large magnet and due to susceptibilities within the body (e.g. air, bone, blood) and their distribution. Inhomogeneities broaden the frequency distribution of the spins and can also cause significant intravoxel dephasing; this is not an issue in RF-refocused (spin-echo) sequences but can reduce signal amplitude considerably in most of the following sequences, particularly the T_2*-weighted acquisitions."

   4.6: "…. this includes frequency and transmitter adjustments to set the basic frequency and the voltage required for the RF coil and amplifier power used, as well as 3D shimming to correct the inhomogeneity of the static magnetic field…. "

2. Figure 12 shows the signal loss due to B1 very clearly. Some mention should be made of this.

   We have included the following section in the section "Representative Results":

   "…. Some distortions in the B_1^+ profile can be observed in the MR images. This is anticipated when moving to higher resonance frequencies [1]; the shorter wavelengths increase destructive and constructive interferences [2,3]. ….."

3. Figure 14: There is almost complete loss of signal due to B1 below the cortex. Appropriate use and placement of **dielectric pads** could improve this substantially.

   We continue the "Representative Results" section with the following text:

   "…. While the B_1^+ pattern cannot be modified for a single transmit element of a given coil, the electromagnetic properties of the surrounding environment may be altered, as has been shown with dielectric padding filled with water [4] or calcium titanate suspensions [5] used at 7.0 T. Geometrically tailored dielectric pads have been shown to be effective at imaging the brain [6,7] and particularly the inner ear [8], a challenging place to image due to inhomogeneities from susceptibility differences between inner ear fluids and bone."

4. Figure 15: 3D SWI seems to be much more B1 sensitive than it should be. There is major signal loss in the center of the brain. There may be a wrong setting for transmit amplitude that is causing this.

   All the representative MR images of the MS case report were acquired using a single channel transmit RF coil on an Siemens 7.0 T MR system. Although this single-channel transmit coil is split into two channels by a power splitter and driven in quadrature mode (0° and 90°), the fixed phase offset between these two channels cannot be adjusted, since this is hardwired to the coil by the manufacturer. Reference power settings are also assigned by the MR system following the adjustments. On Philips and GE scanners, 2-channel transmit coils may be employed, in this case phase and amplitude could be manually adjusted to offset the inhomogeneities.

Apart from pointing out the distortions in the B1+ profile in the "Representative Results" section we also add the following text:

"….To acquire the MR images (Figures 11-14), we used a single channel transmit volume coil on a Siemens 7.0 T MR system in which a manual adjustment of phase and amplitude was not possible to offset the B_1^+ inhomogeneities. Multi-transmit technologies offer the degrees of freedom of parallel transmission required to dynamically modulate the B_1^+ field distribution [9] …"

5. The purpose of each sequence, as it relates to MS pathology should be explained. How does 2D FLASH-ME provide new and different information compared to SWI? QSM is included to capture iron deposition and microbleeds. The importance to MS diagnosis and treatment needs to be better explained. Also, the necessity for both QSM and SWI should be explained. If SWI is being used to detect the central vein sign, this should be stated in the introduction for the sequence.

   In the opening section of each sequence we added more detail regarding the purpose of the acquisition method, as it relates to the MS pathology. As shown in one of the representative results (**Figure 15b**) of our case report, SWI delineates the hypointense rim structure around the lesion that suggests the presence of iron-laden macrophages. We have also included an explanation for using QSM in addition to SWI.

6. The spatial resolution of the DW-EPI does not seem to leverage the SNR of the 7T at 1.95x1.95x2 mm3. A higher resolution should be achievable. Also, the word isotropic spatial resolution is used when it should be specified as in-slice.

   Although compelling, the feasibility of performing in vivo high-resolution diffusion MRI is still limited in practice, especially for clinical studies at 7.0 T. The increased scan time required to compensate for the reduced SNR because of the increased spatial resolution to [1×1×1]mm^3 [10] is not compatible with patient examinations that might include other equally important sequences. While increased power deposition (SAR) is a significant challenge at higher resolutions, the shorter T_2^* and stronger B_0 inhomogeneity at 7.0 T that are already a cause of image blurring and distortion artefacts for EPI, an increase in the matrix size is likely to increase the propensity to distortion artefacts due to lengthening in the echo train length. Reducing the voxel size at 7.0 T is not always beneficial and artefacts could be an additional source of bias [11]. We believe that the benefit of increasing spatial resolution of the DW-EPI at 7.0 T does not outweigh the risk of introducing bias in the data due to blurring and distortion artefacts.

   We changed "isotropic spatial resolution" to "spatial resolution".

Minor Concerns:

7. In the introduction and discussion, some mention of how MS imaging could be improved with greater coverage afforded by the parallel transmit (pTx) Nova Medical coil would be good to include.

   As mentioned in point 4 we have included the advantage of parallel transmission in the "Representative Results" section. We have also included the following text in the introduction:

   "Transmission field (B_1^+) inhomogeneities that are an adverse attribute of the ^1H radio-frequency used at ultrahigh magnetic fields [1] would benefit from multichannel transmission using parallel transmit (pTx) RF coils and RF pulse design approaches that enhance B_1^+ homogeneity and thus facilitate uniform coverage of the brain [9]."

8. Much of the detail provided for the scan protocol is for any standard MRI scan. Perhaps some of the steps may not be necessary to include.

   We have reduced some of the steps that were redundant or those too specific to Siemens MR systems.

9. It would be good to make some mention in the discussion of extending coverage into the brain stem and spinal cord through new coils and pTx. For MS it would be a very important future direction given prevalence of MS lesions in these regions.

   As mentioned in point 7 we now include the advantage of parallel transmission in the introduction and in the representative results section. Additionally, we add a sentence on the benefits of parallel transmission for spinal cord imaging within a new concluding paragraph in this section:

   "…. Aside from brain lesions, lesions in the spinal cord frequently affect MS patients causing motor, sensory and autonomic dysfunction. However spinal cord imaging, particularly at 7.0 T, is technically challenging [12]. Further developments in parallel transmission and parallel imaging are warranted to overcome the hurdles of distorted B_1 field profiles [13]. …"

10. MP2RAGE may be a work in progress sequence. Might be good to cite the developer.

    We had already cited the original publication on MP2RAGE by Jose Marques and colleagues [14]. We now also included that: ***"The open-source MP2RAGE code is available from the developer: https://github.com/JosePMarques/MP2RAGE-related-scripts"***

11. 4.52: The fact that the b value is set to 0 here is confusing. Perhaps the purpose of each of these acquisitions (e.g. B0 correction) needs to be stated.

    We agree with the reviewer that an explanation is necessary. We have added the following sentences to the introduction of this sequence:

    "DW-EPI is commonly associated with geometric distortions that appear as stretched or compressed pixels in the acquired image. In order to compensate for this, reversed phase gradient approaches have been introduced, in which the same slice is acquired twice using opposite phase encoding (PE) polarities [15,16]. The opposite spatial distortion patterns can be aligned and the images combined using registration tools. For distortion correction, the same image is acquired with a reversed PE direction but without diffusion weighting, hence a reduction in acquisition time."

References:

1 Vaughan, J. T. *et al.* 7T vs. 4T: RF power, homogeneity, and signal-to-noise comparison in head images. *Magnetic Resonance in Medicine.* **46** (1), 24-30, doi:https://doi.org/10.1002/mrm.1156, (2001).

2 Van de Moortele, P. F. *et al.* B(1) destructive interferences and spatial phase patterns at 7 T with a head transceiver array coil. *Magn Reson Med.* **54** (6), 1503-1518, doi:10.1002/mrm.20708, (2005).

3 Collins, C. M., Liu, W., Schreiber, W., Yang, Q. X. & Smith, M. B. Central brightening due to constructive interference with, without, and despite dielectric resonance. *J Magn Reson Imaging.* **21** (2), 192-196, doi:10.1002/jmri.20245, (2005).

4 Yang, Q. X. *et al.* Manipulation of image intensity distribution at 7.0 T: passive RF shimming and focusing with dielectric materials. *J Magn Reson Imaging.* **24** (1), 197-202, doi:10.1002/jmri.20603, (2006).

5 Teeuwisse, W. M., Brink, W. M. & Webb, A. G. Quantitative assessment of the effects of high-permittivity pads in 7 Tesla MRI of the brain. *Magnetic Resonance in Medicine.* **67** (5), 1285-1293, doi:https://doi.org/10.1002/mrm.23108, (2012).

6 van Gemert, J., Brink, W., Webb, A. & Remis, R. High-permittivity pad design tool for 7T neuroimaging and 3T body imaging. *Magnetic Resonance in Medicine.* **81** (5), 3370-3378, doi:https://doi.org/10.1002/mrm.27629, (2019).

7 Vaidya, M. V. *et al.* Improved detection of fMRI activation in the cerebellum at 7T with dielectric pads extending the imaging region of a commercial head coil. *Journal of magnetic resonance imaging : JMRI.* **48** (2), 431-440, doi:10.1002/jmri.25936, (2018).

8 Brink, W. M., van der Jagt, A. M., Versluis, M. J., Verbist, B. M. & Webb, A. G. High permittivity dielectric pads improve high spatial resolution magnetic resonance imaging of the inner ear at 7 T. *Invest Radiol.* **49** (5), 271-277, doi:10.1097/rli.0000000000000026, (2014).

9 Padormo, F., Beqiri, A., Hajnal, J. V. & Malik, S. J. Parallel transmission for ultrahigh-field imaging. *NMR in biomedicine.* **29** (9), 1145-1161, doi:10.1002/nbm.3313, (2016).

10 Vu, A. T. *et al.* High resolution whole brain diffusion imaging at 7T for the Human Connectome Project. *NeuroImage.* **122** 318-331, doi:https://doi.org/10.1016/j.neuroimage.2015.08.004, (2015).

11 Lüsebrink, F., Wollrab, A. & Speck, O. Cortical thickness determination of the human brain using high resolution 3T and 7T MRI data. *NeuroImage.* **70** 122-131, doi:https://doi.org/10.1016/j.neuroimage.2012.12.016, (2013).

12 Moccia, M. *et al.* Advances in spinal cord imaging in multiple sclerosis. *Therapeutic advances in neurological disorders.* **12** 1756286419840593-1756286419840593, doi:10.1177/1756286419840593, (2019).

13 Zhao, W. *et al.* Nineteen-channel receive array and four-channel transmit array coil for cervical spinal cord imaging at 7T. *Magnetic resonance in medicine.* **72** (1), 291-300, doi:10.1002/mrm.24911, (2014).

14 Marques, J. P. *et al.* MP2RAGE, a self bias-field corrected sequence for improved segmentation and T1-mapping at high field. *NeuroImage.* **49** (2), 1271-1281, doi:https://doi.org/10.1016/j.neuroimage.2009.10.002, (2010).

15 Holland, D., Kuperman, J. M. & Dale, A. M. Efficient correction of inhomogeneous static magnetic field-induced distortion in Echo Planar Imaging. *NeuroImage.* **50** (1), 175-183, doi:https://doi.org/10.1016/j.neuroimage.2009.11.044, (2010).

16 In, M.-H., Posnansky, O., Beall, E. B., Lowe, M. J. & Speck, O. Distortion correction in EPI using an extended PSF method with a reversed phase gradient approach. *PloS one.* **10** (2), e0116320-e0116320, doi:10.1371/journal.pone.0116320, (2015).